Client
BSEE
Document Title
Ice Scour and Gouging Effects with Respect to Pipeline and Wellhead Placement and Design

WG Reference Number	Client Reference Number (if applicable)
100100.01.PL.REP.003	

Contact

Jorge L. Alba, Senior Consultant
jorge.alba@woodgroupkenny.com
Tel: +1 281 646 4160

Wood Group Kenny
15115 Park Row
3rd Floor
Houston, TX 77084Tel +1 281 675 1000
http://www.woodgroupkenny.com

Revision	Date	Reason for Issue	Prepared	Checked	Approved
0	5/18/2015	Issued for Client Approval	MS	AA/RC	JA
C	5/8/2015	Issued for Client Review	MS	AA/RC	JA
B	3/9/2015	Issued for Client Review	MS	AA	JA
A	2/16/2015	Issued for Internal Review	MS	AA/RT	JA

Revision History (Optional)		
Revision	**Date**	**Comments**
A	2/16/2015	Issued for Internal Review
B	3/9/2015	Issue for Client Review
C	5/8/2015	Issue for Client Review
0	5/15/2015	Issue for Client Approval

HOLDS		
No.	**Section**	**Comment**

Signatory Legend		
Revision	**Role**	**Comments**
0	Prepared	Markella K. Spari, Staff Specialist
	Checked	Aiman Al-Showaiter, Staff Consultant
	Edited	Rhonda Cavender, Senior Technical Editor
	Approved	Jorge Alba, Senior Consultant

Table of Contents

List of Figures

List of Tables

1.0 Introduction

1.1 General

This interim report has been written as part of the requirements included in the Statement of Work in Contract No. E14PC00011 between the Bureau of Safety and Environmental Enforcement (BSEE) and Wood Group Kenny (WGK). The project is entitled "Ice Scour and Gouging Effects with Respect to Pipeline and Wellhead Placement and Design."

The work under this contract is a result of a proposal submitted in response to the Broad Agency Announcement (BAA) E14PS00019 titled: "Arctic Safety of Oil and Gas Operations in the U.S. Outer Continental Shelf."

Refer to Appendix A, Glossary Terms for definitions of many of the terms used throughout this report.

1.2 Project Objectives

The objective of the project is to identify knowledge gaps in ice scour and gouging effects with respect to pipeline and wellhead placement and design in arctic environments.

Three interim reports will be provided for each Task 1, 2, and 3, respectively. The findings of the three tasks will be included in the Final Report, which will be published by BSEE.

WGK has performed the following tasks:

- Task 1 – Literature Review of Field Data
- Task 2 – Literature Review of Test Data
- Task 3 – Literature Review of Numerical Modeling
- Task 4 – Final Report is a compilation of the first three tasks.

1.3 Report Scope

WGK performed a comprehensive literature review on numerical modeling of ice keel/soil/pipeline interaction. Given the complexity of the ice keel-soil-pipe interaction, the development of numerical models capable of fully simulating this interaction is quite challenging. A number of numerical models have been proposed and used over the years. They have increased in sophistication and complexity with time and with the surge in available computation power.

The most commonly used methods comprise the following two approaches:

- Empirical formulations of the subgouge displacement in combination with a simplified structural analysis of the pipeline
- Continuum Finite Element (FE) methods

This report is organized into three main sections. The first section includes a brief introduction of all the modeling parameters involved in the numerical simulations and their related challenges. The last two thematic sections focus on simplified structural spring and continuum medium approaches.

1.4 Abbreviations

Below is a list of abbreviations that are used throughout the report.

ALE	Arbitrary Lagrangian-Eulerian
ASCE	American Society of Civil Engineers
BAA	Broad Agency Announcement
BSEE	Bureau of Safety and Environmental Enforcement
CEL	Coupled Eulerian-Lagrangian
CPU	Central Processing Unit
DOG	Depth of Gouge
EDC	Excavated Drilling Center
FE	Finite Element
FEA	Finite Element Analysis
HP/HT	High Pressure/High Temperature
JIP	Joint Industry Project
OCR	Overconsolidation Ratio
PIC	Particle-In-Cell
PIRAM	Pipeline Ice Risk Assessment and Mitigation
PRISE	Pressure Ridge Ice Scour Experiment

SGD	Subgouge Deformation
SPH	Smoothed Particle Hydrodynamics
WGK	Wood Group Kenny

2.0 Numerical Modeling of Ice Gouging

2.1 Overview

The ice gouging process is a multifaceted, non-linear problem. Advanced numerical analysis plays a significant role in addressing the complexity of the ice keel-soil-structure interaction. Because of the complex interaction between the modeling aspects involved and the challenges related to numerical simulations, the development and validation of numerical models that are capable of fully simulating this interaction have proven to be quite demanding. A brief overview of these aspects and challenges is presented in the following sections.

2.2 Modeling Aspects

In the early 1990s, physical simulations of ice gouging processes provided researchers with the input data basis for numerical simulations. Parametric studies identified the parameters that strongly affect the keel-soil-pipe response. These parameters are attack angle, keel geometry (gouge depth and width), ice strength, soil type, and pipeline and wellhead properties.

2.2.1 Ice

Attack Angle

The influence of the keel attack angle is particularly important to the gouging process. Steeper keels move greater soil volumes into the frontal mound, while shallower keels force most of the soil under and to the side of the indenter. For the same gouge depth and width, a shallower keel will generally result in greater subgouge displacement than a steeper shaped keel.

Keel Geometry (Gouge Depth and Width)

Estimations of ice gouging keel depth and width can be obtained from direct measurements or inferred from seabed surveys. However, repetitive surveys of gouge events in different areas have not been reliable enough to establish correlations between several parameters such as gouge depth, keel geometry, and water depth. The effect of keel geometry on gouge depth is fundamental to understanding the physical processes involved in ice gouging. Numerical studies have focused on simulating recorded laboratory or field testing results, assuming a constant gouge depth. The common practice for investigating the effect of keel geometry is to use an idealized ice keel shape and vary its dimensions.

Ice Strength

Ice is a finite strength material, and the shear failure (fracture) of the gouging ice feature itself could be the limiting mechanism for the gouge depth reached. The selection of an appropriate constitutive law for the continuum ice rubble to be integrated into a numerical model presents a challenging question. As a result, when simulating a steady state gouging process, the ice indenter is generally considered to be rigid.

2.2.2 Soil

Type/Constitutive Model

When assessing the deformation of a pipeline or wellhead caused by ice gouging, determining the response of the soil to the passing ice is critical. A numerical model represents a simplification of the modeled phenomenon by attempting to capture the most relevant mechanisms. The soil itself is a complex, multi-phased material consisting of soil grains and voids. The grains make contact with each other, forming a soil skeleton; the voids are usually filled with water.

Two principal approaches have been adopted to predict the soil response:

- Calibrated functions based on laboratory scaled tests
- Constitutive models

2.2.3 Pipeline

The ultimate goal for all numerical simulations of ice gouge events has been the assessment of ductility demands on the pipeline. Because of the soil-pipe interaction, the predicted burial depth is sensitive to the gouge depth, pipe diameter, relative stiffness, and operation condition (temperature and pressure).

2.2.4 Wellheads

Literature reviews identify a shortage of numerical models that include wellheads in the analysis. This is an important gap that should be bridged with further numerical efforts that include wellheads.

2.3 Numerical Modeling Challenges

Ice gouging problems can be very complex because they involve issues such as large deformations, contact definitions, material nonlinearity, and strain-dependent behavior. The FE method allows a rigorous solution to such complex problems, where analytical solutions cannot be easily obtained. Although a considerable amount of research effort has been devoted to improve solution algorithms over the last decades, challenges still remain.

2.3.1 Large Deformation Problems

Conventional geotechnical numerical modeling has not focused adequately on processes that involve large deformations and strains such as those encountered in an ice gouging event. It is evident that the Finite Element (FE) approach includes many difficulties when solving geotechnical problems with large deformations. Especially troublesome are the occurrence of contact problems and large mesh distortions, which hinder convergence. Mesh distortions associated with Lagrangian approaches prevent engineers from obtaining reliable solutions. Consequently, new types of formulations that combine Eulerian and Lagrangian formulations have been proposed during the last decades. These formulations include the Coupled Eulerian-Lagrangian (CEL) method and the Arbitrary Lagrangian-Eulerian (ALE) method. Meshless methods, including the Smoothed Particle Hydrodynamics (SPH) method, have also been proposed in recent years.

Adaptive FE procedures automatically refine, coarsen, or relocate elements in an FE mesh to obtain a solution with a specified accuracy. Although a significant amount of research has been devoted to adaptive FE analysis, this method remains complex and has not been widely applied to nonlinear geotechnical problems.

2.3.2 Implicit vs. Explicit Schemes

The selection of an iterative scheme is crucial for the convergence of the numerical solution and the validity of the acquired results. The decision depends heavily on analysis type and model characteristics because the two types of iterative schemes available in commercial software—implicit and explicit—are not supported in all solutions.

The implicit method uses a non-iterative time integration procedure that has very small time steps and does not check for solution convergence after every step. An appropriately selected time step (either calculated by the FE program or specified by the user) generally ensures the stability and accuracy of the solution, but it may yield inaccurate results without any warning messages in some analyses that have been set

up incorrectly. Careful model setup, including appropriate mesh refinement and solution control parameters and post-analysis checks, are necessary to ensure the accuracy of the results.

Because of their formulations, explicit solutions provide opportunities to solve problems with a large number of degrees of freedom. Whereas implicit schemes must iterate to determine the solution to a nonlinear problem, the explicit scheme determines the solution without iterating by explicitly advancing the kinematic state from the previous increment. Even though a given analysis may require a large number of time increments, using the explicit method can be more efficient compared to the implicit method, which requires a large number of iterations.

Advanced Eulerian mesh-based continuum models typically use an explicit FE method because of its ability to handle very high deformations and complex contacts (ice-soil and soil-pipe). Another advantage of the explicit scheme is that it requires much less space and memory than the implicit scheme for the same simulation.

2.3.3 Contact Mechanics

In addition to the large mesh distortions discussed previously, contact problems may occur so that a convergent solution often cannot be found. Two types of widely used contact interactions are the kinematic contact method and the general method. The general contact algorithm enforces the use of the penalty methods and is less stringent compared to the kinematic contact method. A further difference between kinematic and penalty contact is that the critical time increment is unaffected by kinematic contact, but it can be affected by penalty contact. The contact surfaces between the Eulerian and Lagrangian domains in numerical simulations are usually discretized using a general contact method.

2.3.4 Constitutive Modeling

Constitutive modeling was developed from many disciplines, and as a result, many different constitutive laws for differing concepts and materials have been proposed. Each model can be valid within its own realm of applicability, and the constitutive equations must be reasonably representative of the material behavior and contain a realistic number of parameters to be calibrated.

2.3.4.1 Soil

The area of greatest model uncertainty is that related to the characterization of soil response, commonly described as a soil constitutive model. Soil is a complex material that shows nonlinear, time-dependent, and often anisotropic behavior when loaded. This behavior can be generally contributed to non-constant stiffness, irreversible deformations, and changes in soil strength as a result of the loading history and pore pressure build-up under loading.

In an ice gouge event, large deformations occur, particularly within the shallow soil layers beneath the ice keel. Historically, this is the area where the greatest discrepancy between measured data and numerical predictions has been observed.

2.3.4.2 Ice

The selection of an appropriate constitutive law to model the behavior of ice rubble as a continuum medium and its integration into a numerical model are major challenges. In addition, an appropriate model for icebergs or other strong ice features interacting with soft-soil seabed scenarios may not be appropriate for first-year ice ridges or other loosely bonded ice features interacting with strong soil seabed scenarios. Glacier or sea ice is a highly heterogeneous material. At low strains, its behavior is ductile, and it is characterized by strain-rate hardening and thermal softening. At high strain rates, it is brittle with sudden material collapse (Jordaan, 2001 [19]; Liferov, 2005 [35]). Envelopes and surfaces describing both ductile and brittle failure are difficult to incorporate into constitutive models for ice. Most of the numerical simulations have treated the ice indenter as rigid to overlook these challenges.

3.0 Simplified Structural Approach

3.1 Overview

Engineering practice has often simplified the complex reality of ice gouging down to an equivalent soil displacement imposed on a pipe/soil system. The pipe/soil system is usually simplified by replacing the components with structural beam elements for the pipe and nonlinear spring elements for the soil. The deformation of the soil mass is modeled by the deformation of three springs with the equivalent stiffness in the axial longitudinal, transverse horizontal, and transverse vertical directions, as described by Committee, 1984 [10]; and O'Rourke and Liu, 1995 [39]. (Refer to Figure 3.1.)

This simplification is derived from the concept of subgrade reaction presented by Winkler, 1867 [55]. The nonlinear, stress-dependent load deformation characteristics of the springs are denoted as t–x, p–y, and q–z curves, representing the behavior of soil in the axial, transverse horizontal, and transverse vertical directions, respectively. The most widely used force-displacement relationships have a hyperbolic or a bilinear form.

The characterization of soil loads on pipelines is performed using three approaches:

1. Use of theoretical soil mechanics to derive equivalent simplified relationships
2. Use of numerical modeling of soil media through FE methods
3. Use of physical models to develop empirical relationships

The practical assessment of the optimal pipeline burial depth for a wide range of modeling parameters (including gouge geometry, pipe geometry, and soil conditions) encountered in pipeline design can only be performed if the ice-soil-pipe interaction is assumed to be decoupled into separate ice-soil and soil-pipe interactions.

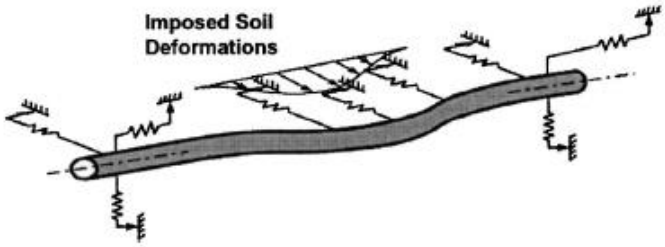

Figure 3.1: Soil-Pipe Interaction using Winkler-Type Model (ASCE, 1984 [2])

The pipeline/soil interaction model accounts for the load transfer mechanisms and the pipeline structural behavior. In general, the current state-of-practice for pipeline/soil interaction analysis uses design guidelines such as the American Society of Civil Engineers (ASCE) [2], which idealize the soil continuum through independent, discrete soil springs.

The soil springs represent a discrete reaction load component of a continuum response through orthogonal reaction forces distributed on the longitudinal and circumferential pipeline axes. The soil spring formulations assume independent load-displacement behavior that does not account for pipeline/soil contact mechanisms (e.g., shear load transfer) and lacks physical significance with realistic, continuum soil behavior (e.g., load-dependent soil response).

The assumption of independent behavior may not be accurate under some conditions, such as limited clearance between the ice keel and the pipe crown or when the subgouge deformation pattern is affected by the presence of the pipe. However, reasonable results have been obtained when comparing measured pipe response to ice gouging (in reduced-scale physical model tests) to simplified structural model predictions.

3.2 Empirical Formulations of Subgouge Deformation

Pipeline deformation is mainly governed by soil displacement, soil stiffness, pipeline stiffness, and pipeline operating conditions. The first parameter, soil displacement, is the most critical factor. The prediction of subgouge deformation is usually based on empirical equations inferred from centrifuge model tests, primarily from the Pressure Ridge Ice Scour Experiment (PRISE) test program [7] [8] [9]. A general assumption is that these empirical equations are conservative and overestimate the soil deformations produced by ice gouging.

Pressure Ridge Ice Scour Experiment

The PRISE joint industry research program investigated the stresses and soil deformations during ice gouging events (Phillips et al., 2004 [43]). It was a proprietary program designed to develop the engineering framework to allow pipeline installation in arctic regions. The program included a series of small-scale physical tests that were conducted in a geotechnical centrifuge to enhance the understanding of soil deformations and ice loads that occur during ice gouging events. A typical configuration of a small-scale centrifuge test is illustrated in Figure 3.2.

A semi-empirical equation for horizontal subgouge soil deformations was derived from centrifuge tests in clay (Woodworth-Lynas et al., 1996 [56]). This is commonly referred to as the PRISE equation.

This combined research effort provided the stimulus and a framework for developing and validating numerical simulations.

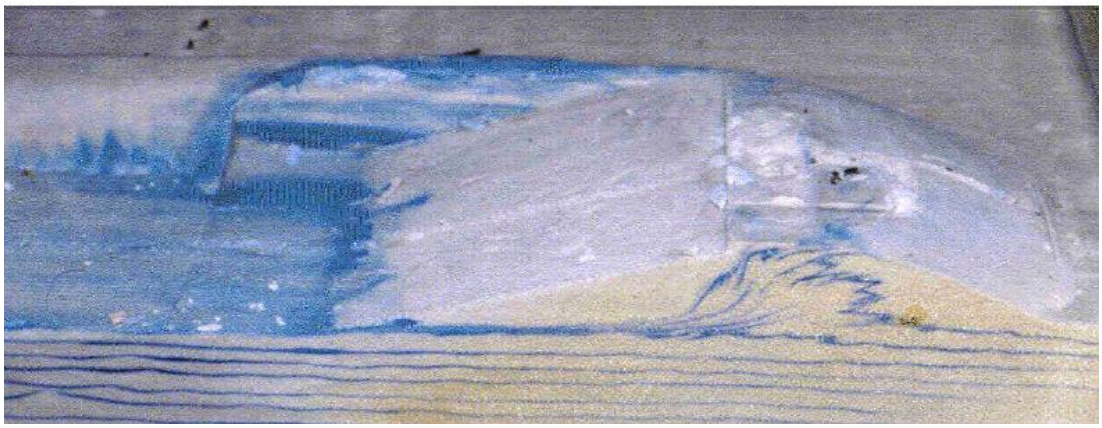

Figure 3.2: Typical Subgouge Failure Mechanism in Sand from PRISE (Phillips, et al., 2005 [44])

3.3 Numerical Studies

3.3.1 C-CORE (1995), Nixon et al. (1996)

The structural approach-based FE software package PIPSOL was used in the PRISE studies to analyze pipeline/soil interaction events and to predict load effects. The PIPSOL formulation is based on an idealized pipeline/soil interaction analysis that incorporates a nonlinear Winkler-type foundation model to define soil reaction loads. The model uses specialized beam elements to account for internal pressure, temperature, axial force, and nonlinear flexural behavior.

The PIPSOL model was adapted for the PRISE study to include the characterization of free field subgouge deformations, nonlinear soil load-deformation relationships, and lateral pipeline/soil interaction behavior (C-CORE, 1995 [6] and Nixon et al. 1996 [36]).

3.3.2 Kenny et al. (2004)

Kenny et al. [27] developed a three-dimensional structural FE model to idealize the continuum pipeline/soil interaction behavior. Kenny modeled the pipeline using 3-node quadratic elements (assuming constant hoop stress) and the soil response using 2-node nonlinear spring elements. Soil response was defined by nonlinear, hyperbolic relationships based on the ASCE (1984) guidelines [2].

The force-displacement relationships, which were defined at the pipeline spring line, accounted for an increased effective burial depth because of the ice feature overburden pressure. The pipeline stress-strain constitutive relationship was defined by isotropic, elastoplastic behavior with a von Mises yield surface and isotropic hardening rule. The stress-strain relationship was defined using the Ramberg-Osgood formulation (refer to the Glossary Terms in Section A.1 of Appendix A).

The work of Kenny et al. established a probabilistic methodology to optimize burial depth requirements for the mitigation of ice gouge hazards.

The authors recommend that future work should:

- Quantify and reduce data and model uncertainty with respect to ice keel/seabed interaction to define geotechnical loads.
- Define load transfer mechanisms for pipeline/soil interaction.
- Establish limit state criteria for a reliability based design methodology.

3.3.3 Peek and Nobahar (2012)

Peek and Nobahar [41] used both a coupled model and an uncoupled model to investigate the necessary burial depth of pipelines. In the uncoupled model, the soil was represented by a set of nonlinear Winkler springs attached to the pipe at one end while the displacement was applied at the other end of the springs. In the coupled models, soil was treated as a 3D continuum medium, and the ALE ABAQUS/Explicit scheme was employed, similar to previous efforts of the same author (Nobahar et al., 2007 [38]).

The added value of this work lies in the comparison of the soil deformation and pipeline response predictions derived by the two different approaches. The authors highlighted that the superposition error caused by adding the subgouge deformations to the soil displacements because of the pipe load that was exerted on the soil was more influential than the coupling errors resulting from directional coupling of Winkler springs in axial, lateral, and vertical directions.

4.0 Continuum Finite Element

4.1 Overview

Continuum models resolve the coupled interactions between ice, soil, and pipe more accurately; therefore, they allow a more realistic representation of the ice gouging process. These models usually predict lower subgouge soil displacements and lower pipeline strain demand compared to soil-spring based structural models, which have the potential to reduce burial depth requirements significantly.

4.2 Lagrangian

In the Lagrangian formulation, time and material coordinates are independent, but the mesh deforms with the material. The nodes' Lagrangian coordinates move with the material (Figure 4.1). Material coordinates of material points are time invariant, and no material passes between elements. Element quadrature points remain coincident with material points; similarly, boundary nodes remain on the boundary. Therefore, boundary conditions and interface conditions are easily applied. These features enable easy free-surface/interface tracking between different materials and simplify the application of boundary conditions. Furthermore, time independency facilitates the treatment of materials with history-dependent constitutive relationships. This formulation makes the modeling of history-dependent materials (e.g., soil) possible.

On the other hand, when a large deformation occurs, the Lagrangian formulation produces mesh distortion. Some extensions of the traditional Lagrangian formulation, such as the Total Lagrangian, the Updated Lagrangian, and the Corotational formulations, have been developed to tackle large deformations. These formulations use mesh update techniques, where computations refer to previous configurations. However, when large deformations occur, the use of a distorted mesh as the reference domain is problematic.

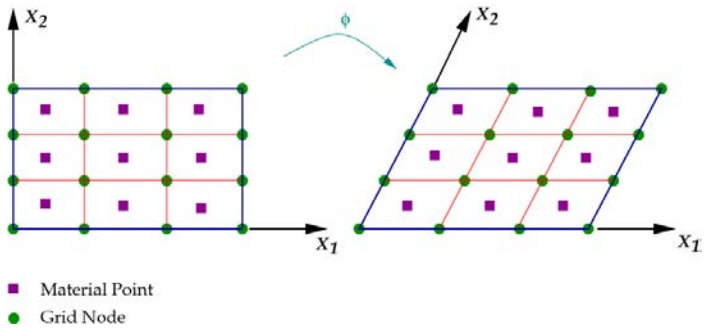

Figure 4.1: Lagrangian Mesh Description

4.2.1 Early Studies

Investigations in the 1990s examined the application of continuum FE methods to analyze ice gouge events. These studies encountered numerical problems such as poor convergence and solution instability caused by severe mesh distortion.

The PRISE research program developed 2D continuum FE modeling procedures for ice gouging, as presented in C-CORE, 1993 [5] and 1995 [6]; Lach, 1996 [30]; Lach and Clark, 1996 [31]; Lach et al., 1993 [32]; Yang et al.,1993 [51]; and Yang and Poorooshasb, 1997 [52].

The preliminary numerical investigations considered an elastic-perfectly plastic soil material model with the Drucker-Prager yield criterion (e.g., C-CORE, 1993 [5]; Yang et al., 1993 [51]; Yang and Poorooshasb, 1997 [52]). The ice keel/seabed interaction was defined by displacement boundary conditions with the assumption of a frictionless interface. These studies evaluated seabed reaction forces, pore water pressure, soil displacement vectors, and plastic strain contours. Surface horizontal displacements of less than 50% of the gouge depth were mobilized before numerical instability halted the analysis. Despite these shortcomings, the analysis provided evidence that Lagrangian, 2D continuum Finite Element Analysis (FEA) modeling was a reasonable engineering tool to model the magnitude and distribution of subgouge deformation profiles in comparison with the PRISE centrifuge experimental data.

C-CORE and Lach and Clark implemented improvements to the numerical modeling procedure to include finite strain formulation and two-phase material behavior based on a modified Cam-Clay model. In addition, they used rigid surface interface elements to account for the ice keel/seabed boundary effects (C-CORE, 1995 [6]; Lach and Clark, 1996 [31]).

4.2.2 Yang and Poorooshasb (1997)

Yang and Poorooshasb [52] conducted one of the early studies on ice gouging that used 2D and 3D FE models to understand the free field and pipe response during ice gouging on drained sand.

The pipeline deflection profiles obtained for both cases did not differ significantly because of the assumption that the pipe moves with the soil without relative slip and that the stiffness of the pipe is relatively small compared to that of soil.

Yang and Poorooshasb observed that the presence of pipeline, with a cover depth equal to the gouge depth, did not influence the free field gouge displacements for small gouge movements. The analysis assumed perfect pipeline/soil contact with no slippage. The 3D FEA identified issues of surcharge clearance mechanisms, but steady-state conditions

were not achieved because of limited mesh size and numerical instability. The analysis, however, provided an indication of the extent and shape of the lateral deformation profiles. The shape and size of the deformation zones is illustrated in Figure 4.2 and Figure 4.3. The authors questioned numerical accuracy because of the severe mesh distortion, and they identified the need for a re-meshing technique.

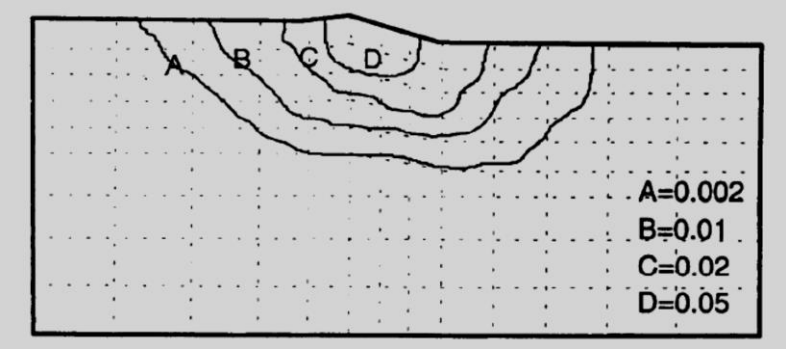

Figure 4.2: Equivalent Plastic Strains Contours (Yang and Poorooshasb, 1997 [52])

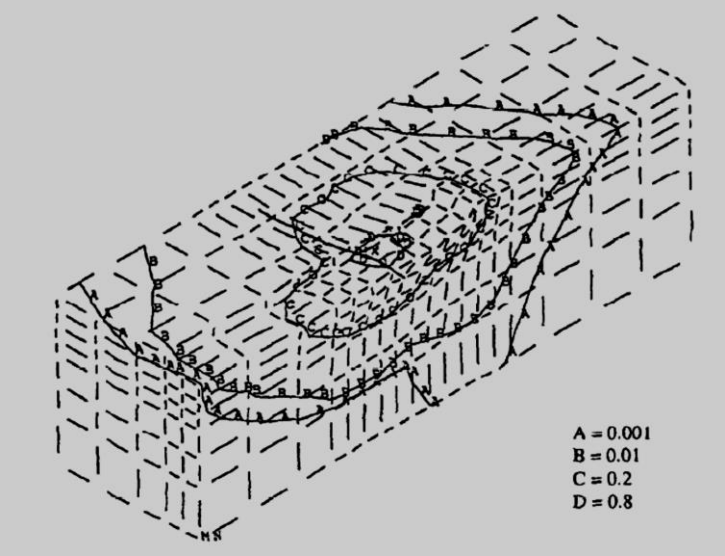

Figure 4.3: Equivalent Plastic Strains Contours (Yang and Poorooshasb, 1997 [52])

4.2.3 C-CORE (1998), Phillips et al. (2004)

The earlier PRISE investigations using 2D FEA were extended to include the simulation of ice gouge events in dilatant soil such as sand or compact silt. A configuration of the model is shown in Figure 4.4. Ice keel horizontal translations of ten gouge depths were achieved. A Mohr-Coulomb soil model was adopted for a parametric study that

examined the variation of elastic modulus with confining stress, friction angle, dilatancy angle, gouge depth, soil cohesion, permeability, and ice keel interface friction angle. The study concluded that the elastic modulus of the soil strongly influenced the subgouge deformation results. Numerical analyses revealed trends that confirmed the magnitude and extent of the subgouge deformations that were observed in the centrifuge tests. The plastic deformation zone extended to a few gouge depths and was consistent with other studies conducted under PRISE. In comparison with the previous FE studies on soft clays conducted by the same researchers, the numerical analysis for dilatant materials was less successful in supporting the PRISE centrifuge experimental data.

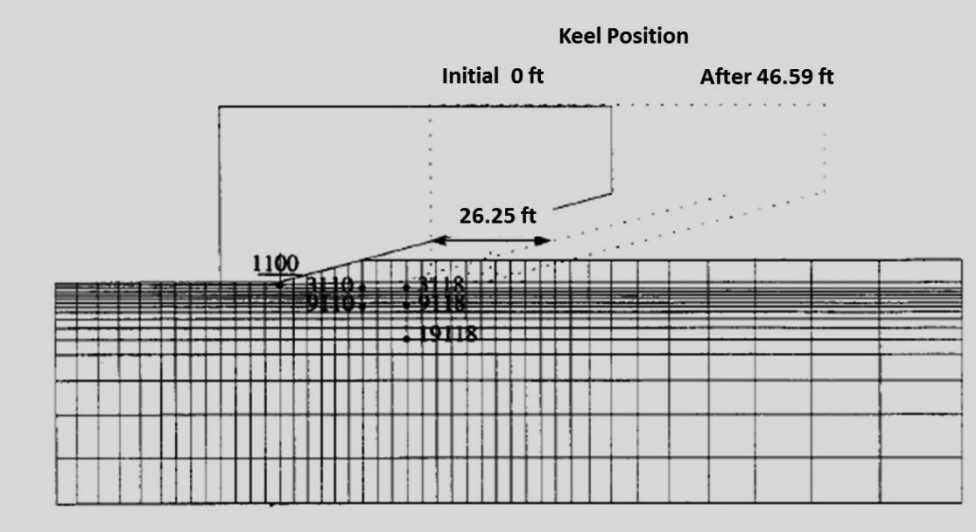

Figure 4.4: Finite Element Mesh for Scour Depth (C-CORE, 1998 [8])

4.2.4 Nobahar et al. (2004)

Nobahar (2004) [37] performed two-dimensional simulations of the seabed scouring problem using the commercial FE package ABAQUS/Explicit. The seabed was modeled as undrained clayey material using the total stress concept with a simple von Mises yield criterion as the plasticity model. A constant undrained shear strength of 3.63 psi (25 kPa) and an initial embedment depth to reach the required scour depth were assumed. Both scouring in the absence of a buried pipe and coupled scouring and soil-pipe interaction were performed in two dimensions.

The objective of the research was to compare monolithic coupled versus staggered analyses results with respect to keel-soil-pipe interaction. The analyses indicated that an ice gouge event with a keel depth approaching or even exceeding pipeline cover depth does not necessarily lead to a catastrophic failure of the pipeline.

4.3 Arbitrary Lagrangian-Eulerian (ALE)

4.3.1 Overview

During the ice gouging process, the soil medium undergoes very large deformations in front of and underneath the ice feature. Preforming FE analyses without the mesh adaptive technique resulted in severe numerical difficulties as reported by Kenny et al., 2005 [28]; Lach, 1996 [30]; Lach and Clark, 1996 [31]; and Yang and Poorooshasb, 1997 [52]. The most important difficulty was associated with element distortion that occurs caused by large deformations or two-dimensional model idealizations or both.

The ALE approach has been used to solve complex technical problems in a variety of engineering fields such as fluid-structure interaction, large deformation solid mechanics (Donea et al., 2004 [12] and Wang and Gadala, 1997 [54]), and geomechanics with respect to nonlinear, large deformation problems involving strain localization (e.g., Zienkiewicz et al., 1995 [53]).

In the ALE formulation, the nodes of the computational mesh may be moved with the continuum in normal Lagrangian fashion or held fixed in the Eulerian manner. The nodes can also be moved in some arbitrarily specified way to give a continuous rezoning capability. Because of this freedom in nodes movement, the computational mesh offered by the ALE description provides better handling of the greater distortions of the continuum than the purely Lagrangian method and more resolution than that afforded by a purely Eulerian approach (Donea et al., 2004 [12]).

It has been noted that these advanced numerical procedures have some restrictions with respect to element selection (i.e., type, order) for non-adaptive mesh interfaces where there is a change in the material properties (e.g., native and backfilled soil at a trench interface). Also, soil plasticity models are limited to single-phase material behavior (i.e., no pore pressure effects).

In the ALE method, the analysis undergoes three major steps. In the first step, a standard Lagrangian FE analysis is conducted. In the second step, the FE mesh is remapped based on smoothing criteria. The remapping algorithms can be based on the stresses and the deformations obtained in the previous time step or on the mesh topology. The third step in the ALE approach is the advection phase. In this step, the discretized strain, mass, and momentum parameters are computed for each node of the new mesh using the laws of conservation of mass and momentum. An example of ALE remapping in comparison to the Lagrangian and Eulerian scheme is shown in Figure 4.5.

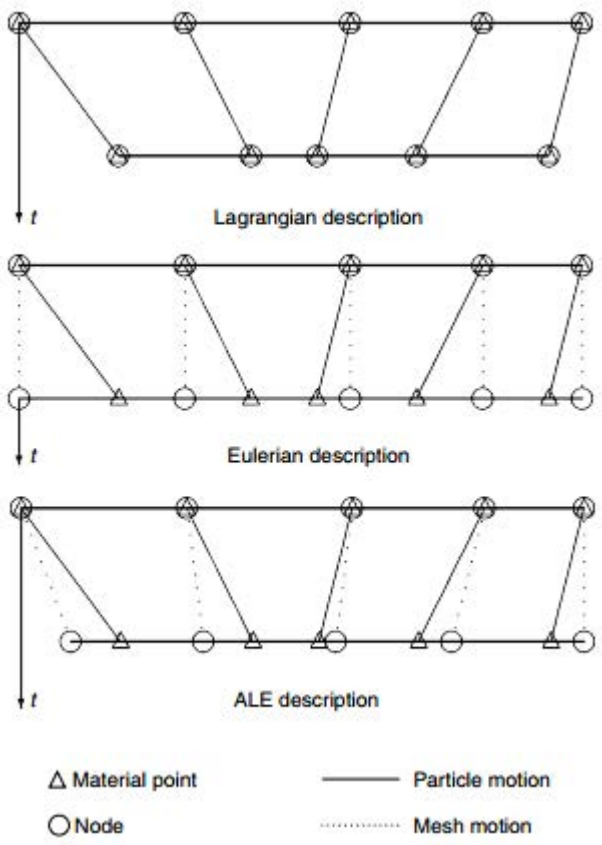

Figure 4.5: One-dimensional Example of Lagrangian, Eularian and ALEl Mesh and Particle Motion (Donea et al., 2004 [12])

4.3.2 Kenny et al. (2007)

Kenny et al. [29] implemented an ALE modeling approach using the software package ABAQUS/Explicit to assess the magnitude and extent of subgouge deformations. This study modeled soil plasticity using von Mises criterion and total stress analysis. The test conditions consisted of a rigid ice keel gouging through a deformable clayey seabed with an undrained shear strength of 3.63 psi (25 kPa). (Refer to Figure 4.6.)

The gouge depth and width were 4.79 ft. (1.46 m) and 32.81 ft. (10 m) respectively, with an attack angle of 15° to the horizontal.

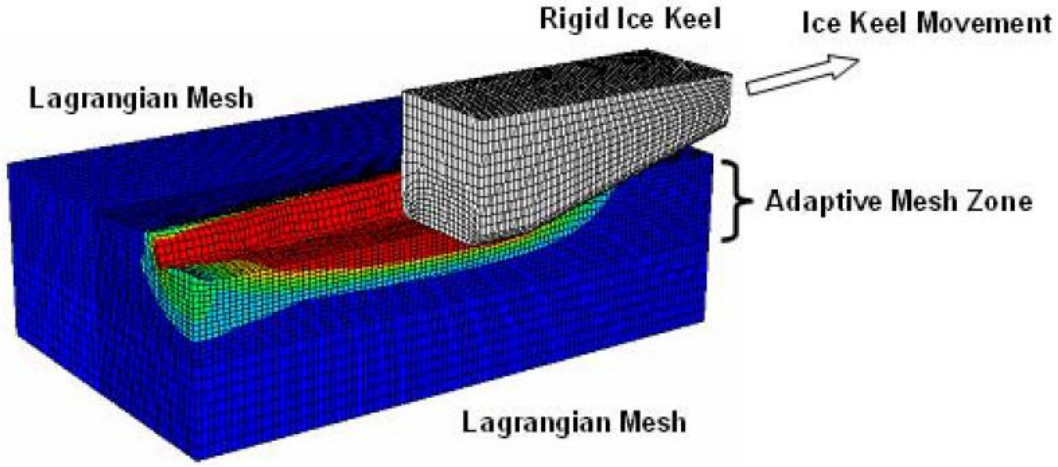

Figure 4.6: Finite Element Model of an Ice Gouge Event (Kenny et al., 2007) [29])

The authors monitored the magnitude and extent of subgouge deformations by defining an array of tracer particles as presented in Figure 4.7.

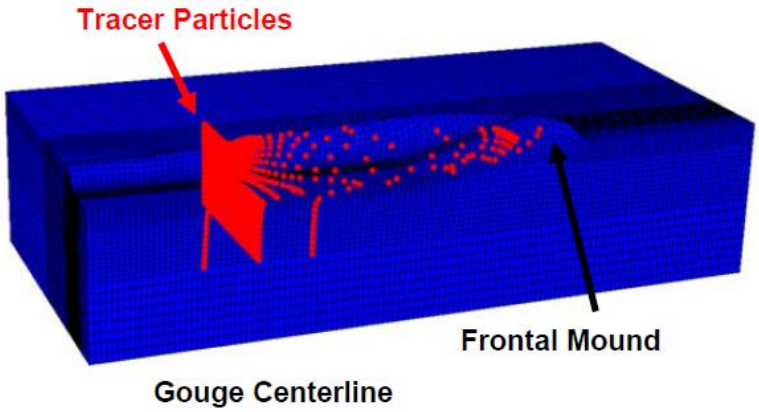

Figure 4.7: Tracer Particle Array Used to Characterize Subgouge Deformations (Kenny et al., 2007 [29])

Figure 4.8 presents a comparison of the vertical profile of subgouge deformations with a depth beneath the ice keel as predicted by the ALE procedures with the centrifuge modeling data.

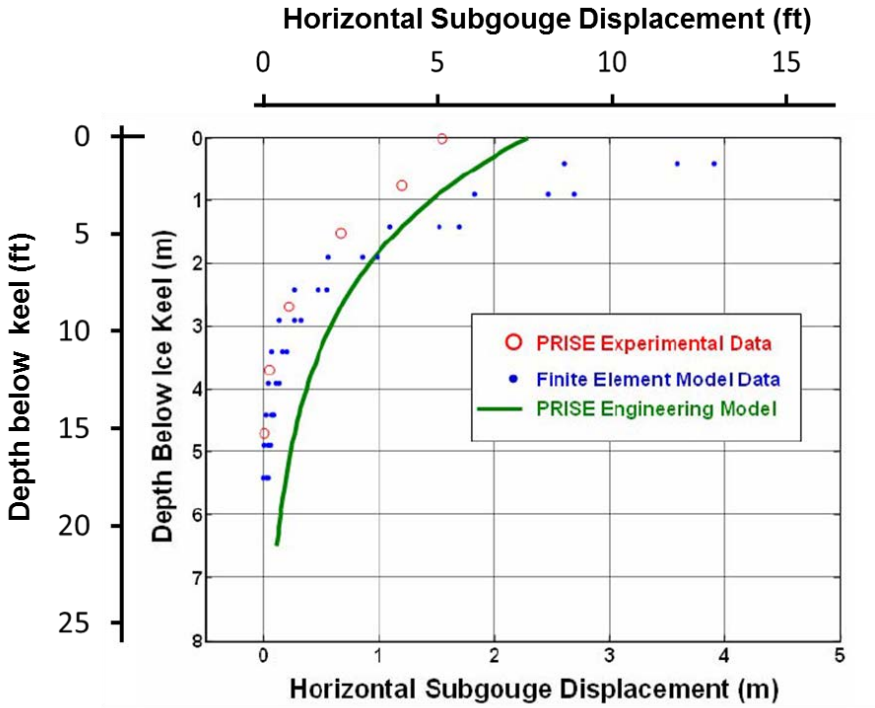

Figure 4.8: Vertical Profile of Subgouge Deformations from Numerical and Reduced Scale Centrifuge Modeling Studies (Kenny et al., 2007 [29])

The soil failure mechanism observed during the numerical solutions (refer to Figure 4.9) involved the build-up of soil surcharge in front of the advancing ice keel, a rupture surface through the seabed penetrating the mudline, a dead wedge trapped adjacent to the inclined ice keel face, and subgouge deformations extending beneath the base of the ice keel. These findings were consistent with the soil failure mechanism as described by Been et al., 1990 [4].

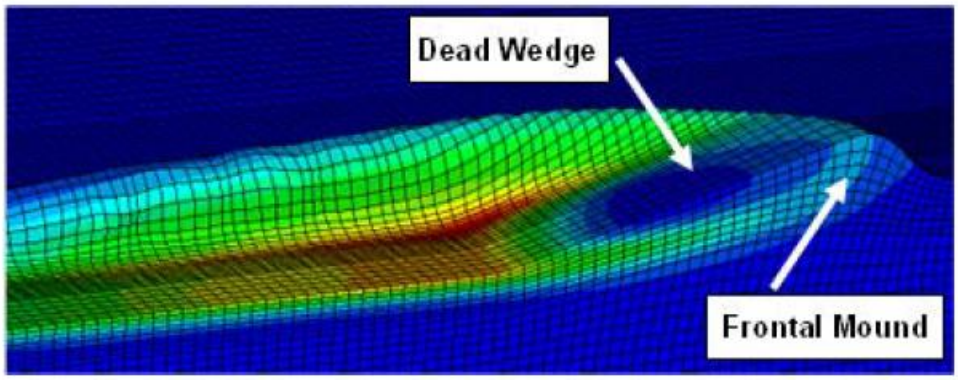

Figure 4.9: Distribution of Equivalent Plastic Strains (Kenny et al., 2007 [29])

4.3.3 Nobahar et al. (2007)

The study of Nobahar et al. [38] presents an explicit continuum FEA of pipe/soil and pipe/soil/ice keel and compares the results from continuum FE with a Winkler-type analysis for the same analyzed problem. The study considered ice features with an attack angle of 30° crossing the pipeline path in the transverse direction (see Figure 4.10). Nobahar et al. evaluated the pipe/soil contact interface through a frictional contact surface allowing finite sliding and separation between the two surfaces based on Coulomb frictional criterion.

The authors noted that both the ice feature's attack angle and the interface friction affected the failure mechanism of the soil and the depth of the failure plastic wedges. They also observed that soil failure occurs at lower load levels for undrained loading of cohesive clayey soil when it is loaded simultaneously in various directions compared with independent loading in a single direction. The pipeline responses in terms of stresses and strains were lower than those estimated using a conventional Winkler-type structural approach and the decoupled pipe/soil/ice keel interaction approach. Figure 4.11 shows an estimation of horizontal and vertical forces mobilized during gouging through two clayey seabeds (one soft and one stiffer). Nobahar et al. concluded that the structural approach provided reasonably conservative results for the studied parameters and soil inputs, but the coupled pipe/soil behavior requires additional studies and verification.

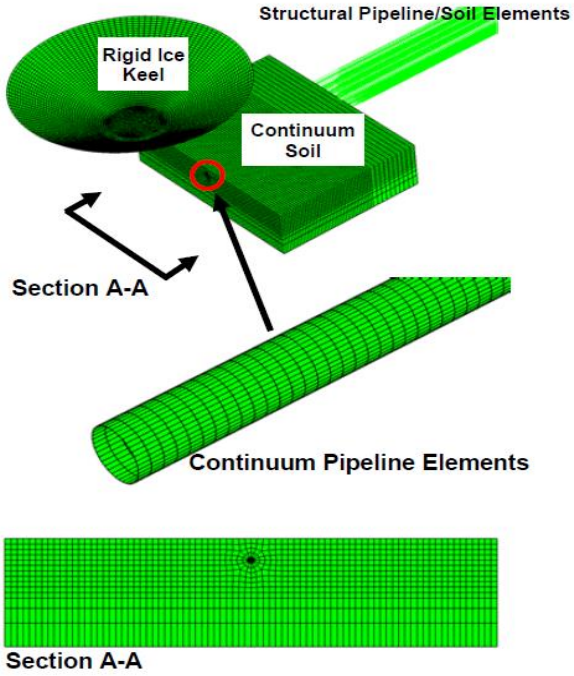

Figure 4.10: Fully Coupled Ice Keel/Seabed/Pipeline Interaction Model (Nobahar et al., 2007 [38])

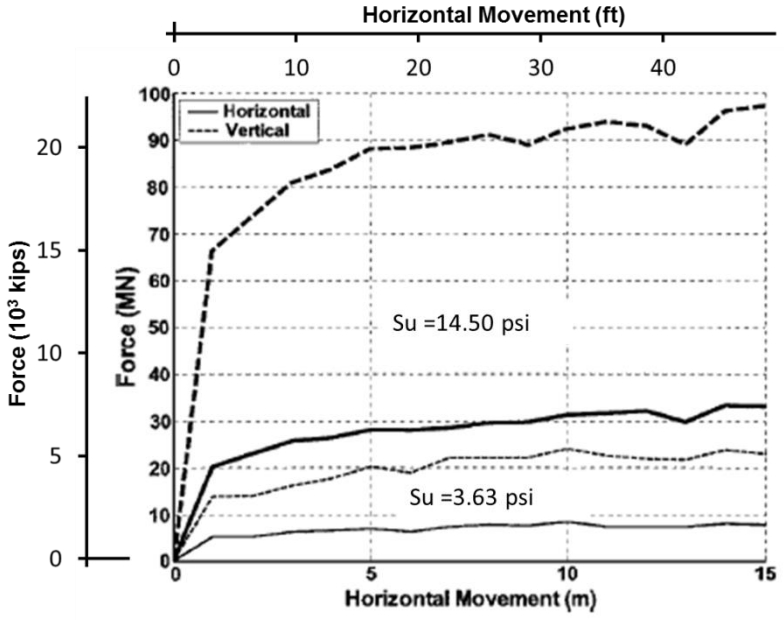

Figure 4.11: Horizontal and Vertical Gouging Forces for 4.92 ft. (1.5 m) deep gouge for Soil Types I and II (Nobahar et al., 2007 [38])

4.3.4 Konuk et al. (2005a)

Konuk et al. [26] developed an FE model using an LS-DYNA explicit model. The researchers used a CAP model (constitutive model where shear and compaction surfaces are combined to form a smooth continuous surface) for the soil, assuming undrained conditions. The ice ridge was idealized as a rigid conical indenter with the ridge angle varying from 15° to 45° (refer to Figure 4.12). Scour width was 49.21 ft. (15 m), and the size of the model ensured negligible boundary effects and steady state.

The results indicated a logarithmic relationship between the subscour deformation and the ridge angle because the change in subscour deformation from 30° to 15° (angle) was exponentially higher than the change from 45° to 30° (angle). Figure 4.13 shows a snapshot of the deformed mesh for the 45° (angle) case. On the other hand, the subscour magnitude increased proportionally with the scour depth. The vertical reaction force on the indenter increased by a rate similar to the rate of increase in subscour deformations, suggesting that the reaction force applied by the ice sheet was independent of ridge geometry and that the buoyancy contribution was relatively small.

The results showed that at lower ridge angles, the subscour deformations and the ice-soil reaction forces were very sensitive to the ice ridge angle. The authors implied a correlation between the scour depths and the ridge angles (deeper scours are formed by higher slope ridges), but they highlighted the need to verify findings against field testing.

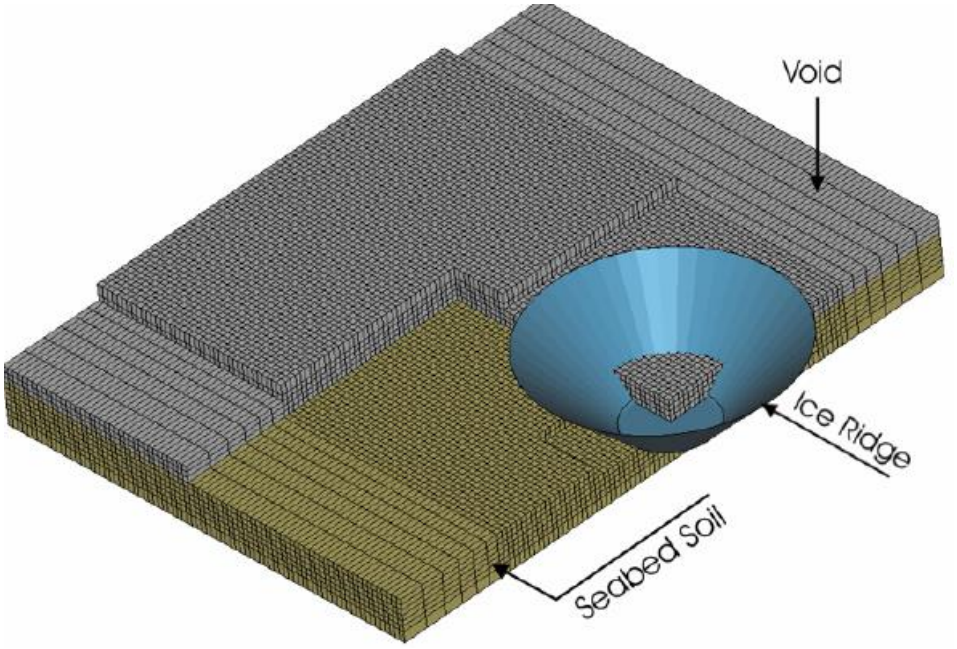

Figure 4.12: Illustration of the FE Model (Konuk et al., 2004a [24])

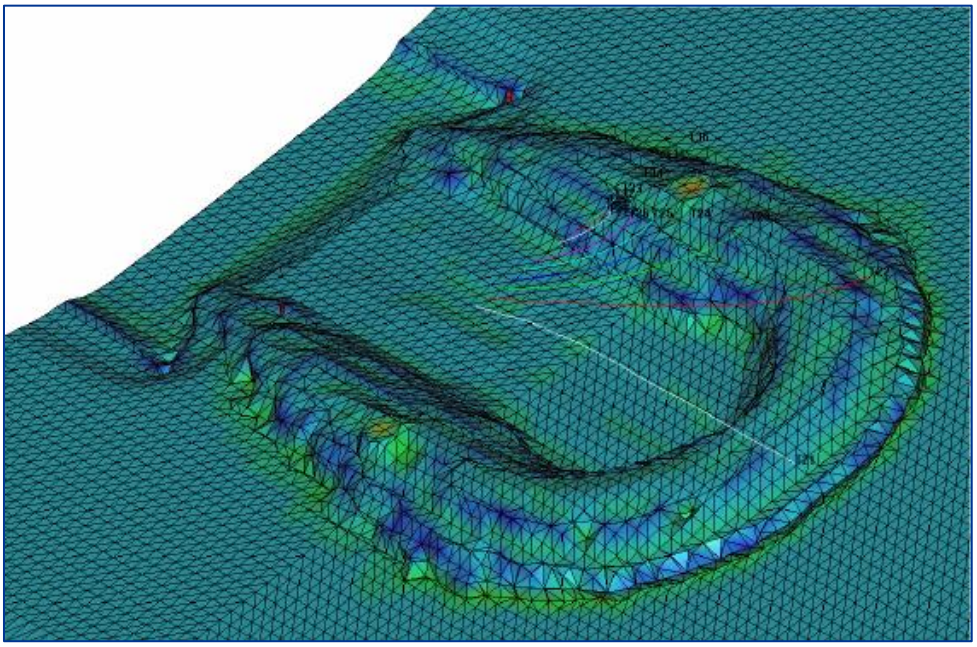

Figure 4.13: Typical Output from FE Model with 45° Ice Ridge (Konuk et al., 2004a [24])

4.3.5 Konuk et al. (2004b)

Konuk et al. [25] conducted an earlier study that focused on the effects of the pipeline trench on the scour process and the forces transmitted to the pipeline.

The authors used two versions of a conical indenter in the study. Both indenters had a width of 49.21 ft. (15 m), and the ridge angles were 30° and 45°, respectively. A 36-inch diameter pipe was modeled as a rigid structure and was kept stationary at its original position. Soil-pipe contact was defined (similar to the soil-ice contact) using penalty functions. Two types of soils that were somewhat softer than the ambient seabed soils were used to cover the pipeline and fill the trench modeled with the CAP soil constitutive model.

Konuk et al. observed the significance of the trench in the soil deformation profile (refer to Figure 4.14 and Figure 4.15), which generated a very different discontinuity in the presence or absence of the pipe and trench. The horizontal loads were cyclic, varied gradually, and not significantly affected by the ridge angle. The force on the pipe increased until the front of the ice ridge reached the pipeline axis; it decreased at the same rate of increase and eventually became negative. The horizontal loads pushed the pipeline forward and then backward by about the same magnitude. Refer to Figure 4.16.

In this study, the pipe was fixed and rigid, implying that peak calculated loads in the ALE FE model were an 'upper limit,' depending on the soil properties. However, these loads were somewhat lower than the loads calculated by the Winkler (structural) models. Intuitively, the stiffer the infill soil is, the higher the horizontal loads experienced by the pipeline will be. Similarly, vertical pipeline loads were significantly higher for the stiffer soil.

The authors recommended a more detailed study of infill properties and the analysis of unburied flexible pipe, which could be beneficial for optimum design protection purposes.

Figure 4.14 presents the deformation profiles produced by the 30° and 45° angle indenter, with and without trench, and using two different types of soil for trenching material. The effect of the trench to the pipe response is apparent.

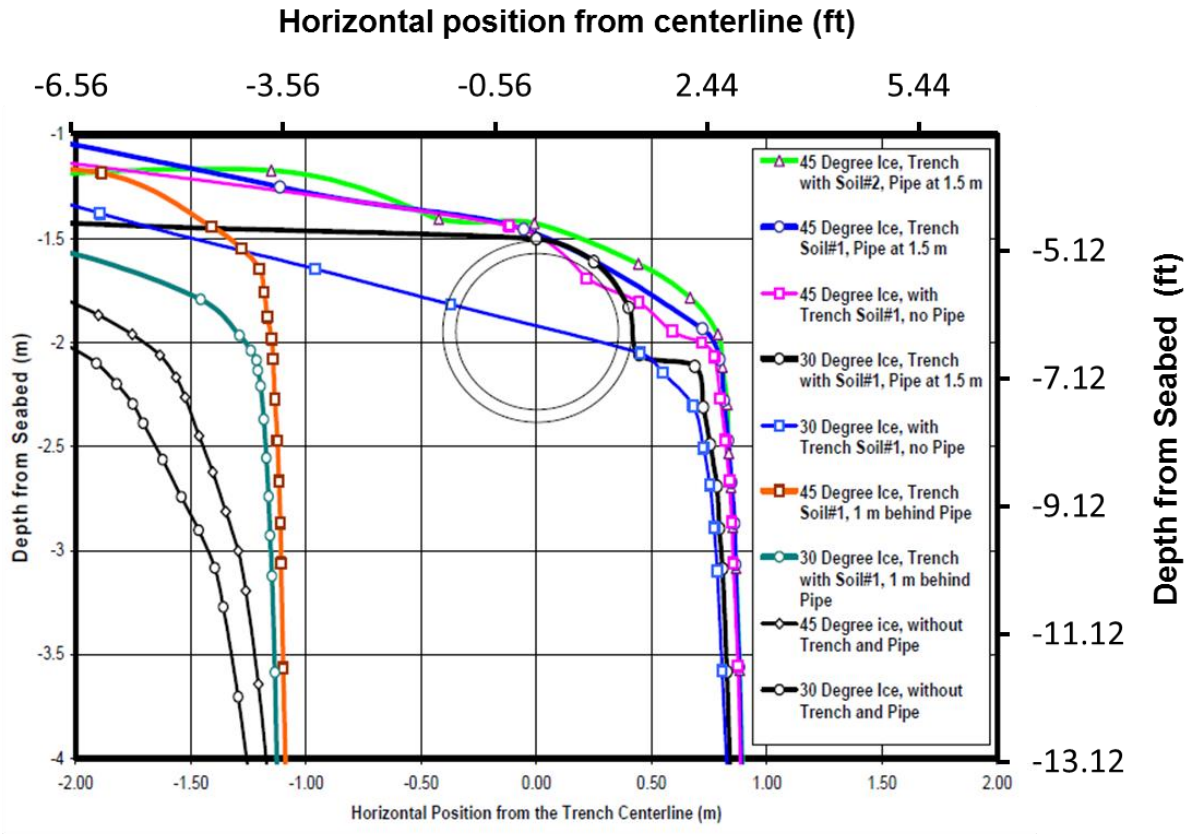

Figure 4.14: Comparison of Soil Deformation Profiles (Konuk et al., 2004b [25])

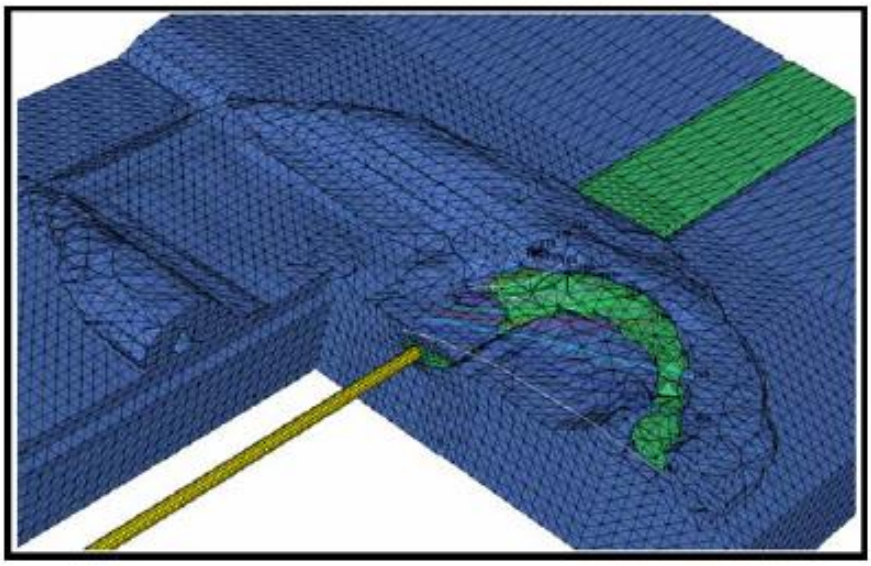

Figure 4.15: Visualization of Typical Output from the ALE FE Model – 45° Ice Ridge (Konuk et al., 2004b [25])

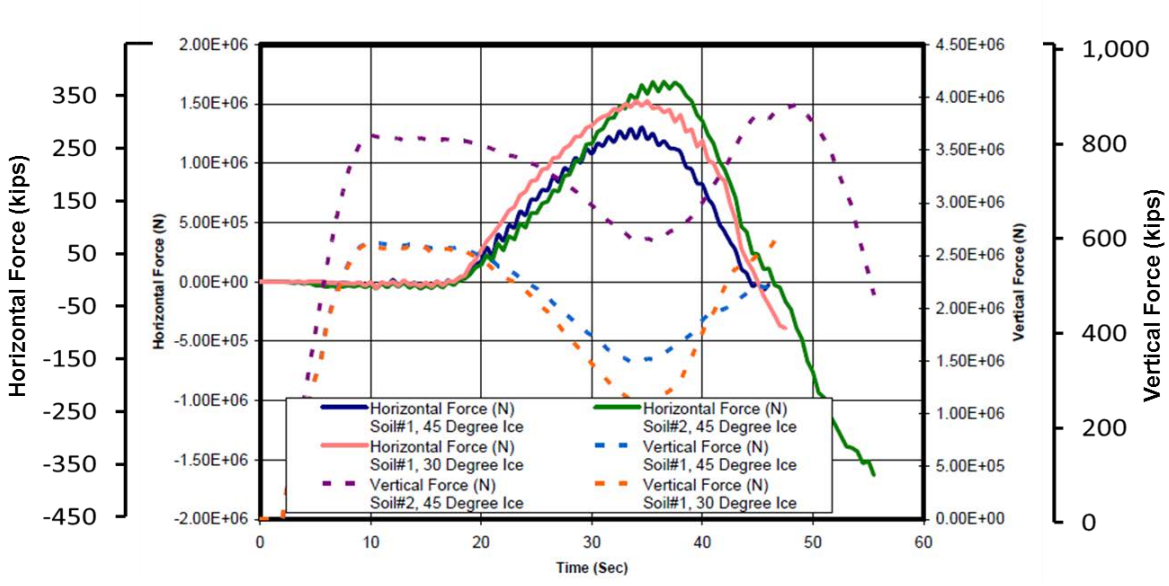

Figure 4.16: Vertical and Horizontal Pipe Forces (Konuk et al., 2004b [25])

4.3.6 Fredj et al. (2008)

Fredj et al. [16] conducted a parametric study to define the governing parameters for High Pressure/High Temperature (HP/HT) pipeline design. The effect of the operating pressure and thermal loads on the pipeline response was studied.

Comparison of the two scenarios indicates differences in the maximum pipe displacement; in the case of an operating pipe, it is greater than the cold unpressurized pipe (130% in vertical direction and 150% in lateral). Bending moment and curvature showed the same trend. Explicitly, axial forces developed in an operating pipe caused by pressure and thermal loads have an important influence on the pipeline's response in terms of stresses and strains. The results presented in Figure 4.17 show that the maximum pipeline displacement increases with the gouge width. However, plastic strains do not follow the same trend.

The ALE model and two Winkler springs models were used to simulate a single ice scour event. One spring model used pipe elements, and the other used shell elements. Results derived from the two different formulations were in good agreement with each other. However, compared to the continuum model, both formations predicted higher displacements for narrower gouge width (see Figure 4.18).

The research concluded that for a given pipe geometry and operating condition, there is a critical gouge width that maximizes pipe bending moments and strains. The influence of trench bottom imperfections was also assessed, indicating that pipeline misalignments of 0.98 ft. (0.3 m) in the vertical or lateral directions do have a significant impact on pipe response.

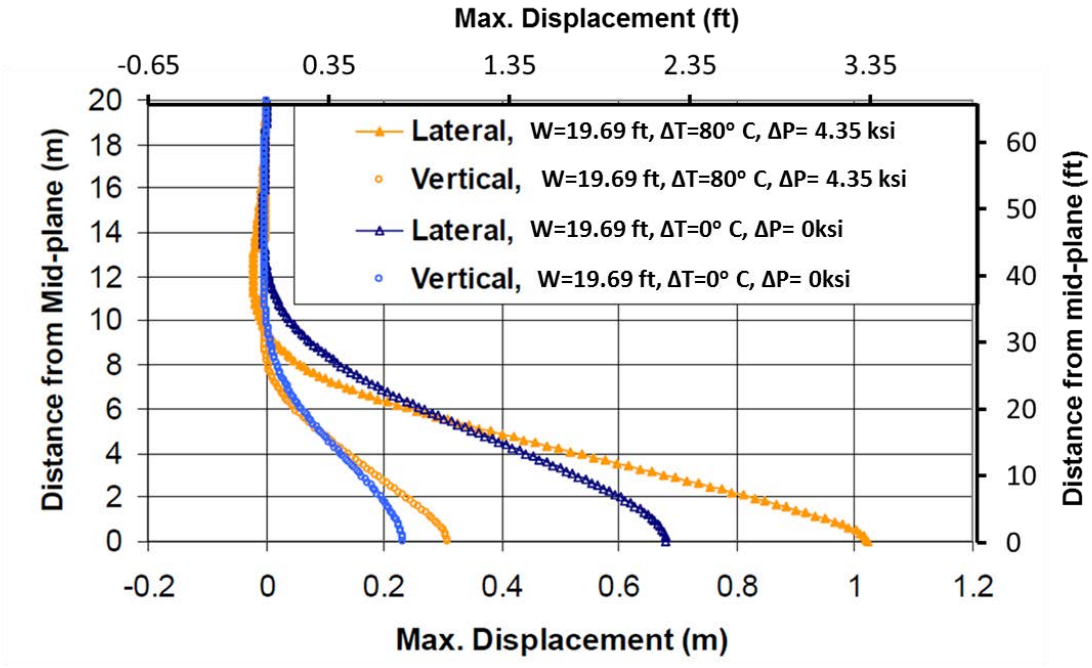

Figure 4.17: Comparison of Lateral and Vertical Displacement Pressurized vs. Unpressurized (Fredj et al., 2008 [16])

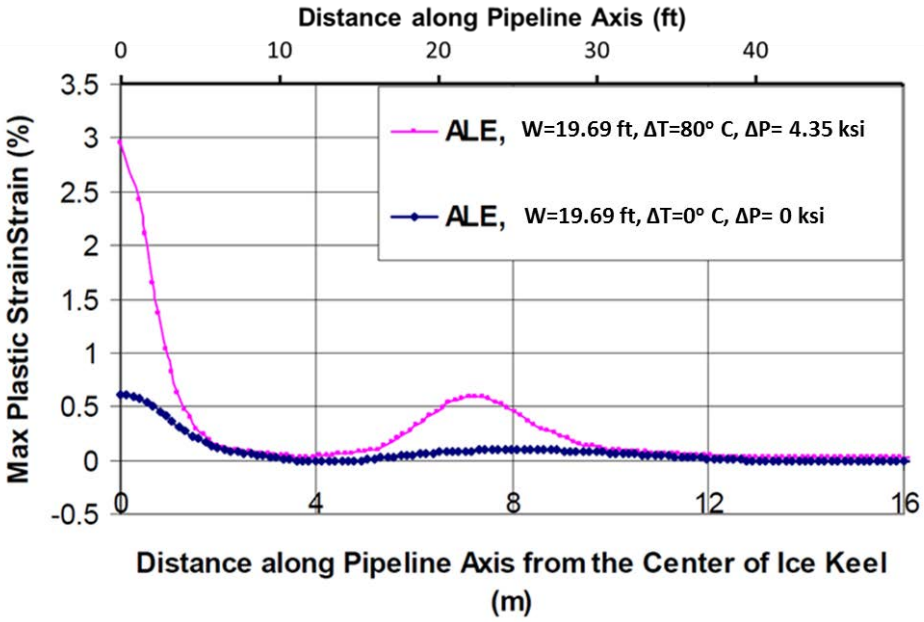

Figure 4.18: Comparison of Plastic Strain Pressurized vs. Unpressurized (Fredj et al., 2008 [16])

4.3.7 Eskandari et al. (2010, 2011)

Eskandari et al. [13] [14] developed a 3D FE model in ABAQUS/Explicit to simulate the ice gouging events in sand as part of the Pipeline Ice Risk Assessment and Mitigation (PIRAM) Joint Industry Project (JIP). The focal point was a realistic stress-strain behavior that was based on the critical state soil mechanics using the constitutive model NorSand.

The NorSand model applies two principles:

1. A unique locus exists for critical state in the void ratio-stress space.
2. The soils move toward the critical state as the shear strain evolves.

This study used the volume constraint method and extended the NorSand critical state model to simulate the undrained behavior of soils. The rigid keel was idealized as a conical frustum with a diameter of 32.81 ft. (10 m) at the base and an attack angle of 30° (Figure 4.19). The soil had a maximum shear stress of 21.75 psi (150 kPa). A friction coefficient μ of 0.2 was chosen for the keel roughness, and the keel base was at a depth of 3.28 ft. (1 m). The deformations and associated reaction forces (vertical, horizontal) were different from those of Phillips and Barrett, 2011 [46] mainly due to the difference in the assumed keel roughness. The results of the analyses were in good agreement with triaxial laboratory tests as published by Jefferies and Been, 2006 [18].

The study investigated the mesh dependency of the ice gouging model using the critical state model NorSand and the two mesh densities. The results observed were scarcely dependent on the selected levels of discretization (Figure 4.20).

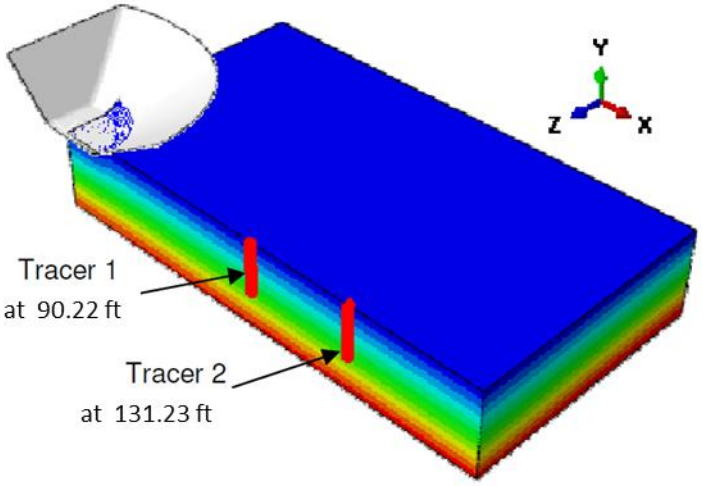

Figure 4.19: Keel and Soil Assembly in FE Model (Eskandari et al., 2011 [14])

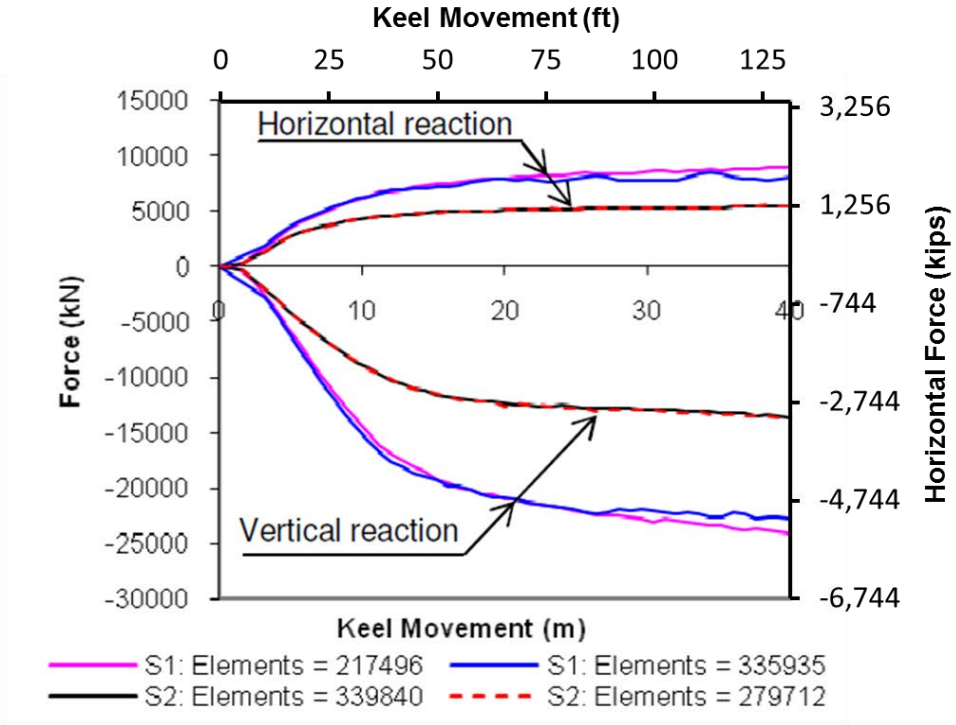

Figure 4.20: Mesh Dependency in NorSand (Eskandari et al., 2011 [14])

Figure 4.21 shows the response of vertical keel reaction after 131.23 ft. (40 m) of keel displacement, depending on the critical state ratio, M_{tc} and state parameter, ψ. The reactions increase with both soil strength and initial sand density.

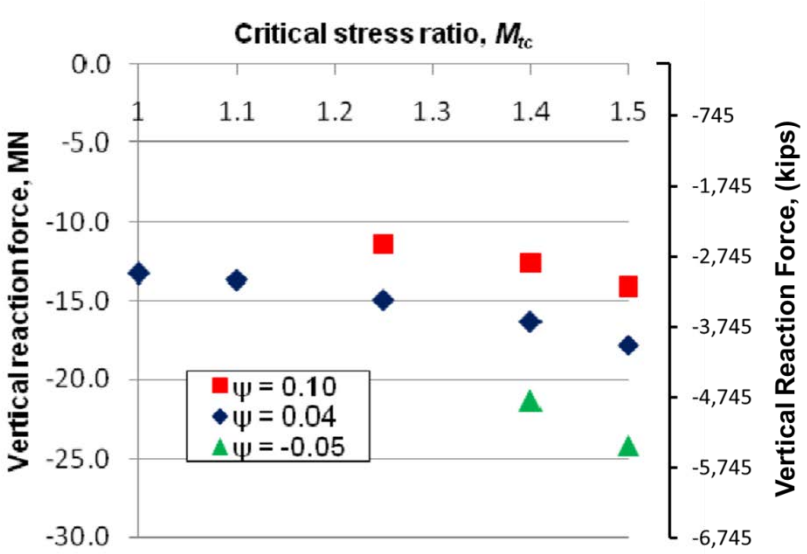

Figure 4.21: Variation of Vertical Force with Critical State Ratio M_{tc} and State Parameter ψ (Eskandari et al., 2011 [14])

The preliminary analyses of Eskandari et al. showed that the NorSand model is capable of predicting ice gouging behaviour, but further study is required to calibrate the model performance.

4.3.8 Eskandari et al. (2012)

This Eskandari et al. study [15] focused on model output results such as keel reaction forces, subgouge deformation, frontal mound height, and failure mechanisms. Among these outputs, the subgouge deformation is consequential because the main target of the ice/soil study was the development of a categorical understanding to determine the optimum burial depth of offshore pipelines.

This model is identical to the medium-sized meshed model of the Phillips and Barrett, 2011 [46] study, with the exception that an ALE formulation was used instead of a CEL formulation.

The state parameter and the critical friction angle are the soil parameters chosen for sensitivity analyses. Other parameters whose significance was also assessed are keel attack angle and gouging depth. The increase of the gouging depth directly affected the subgouge deformation, extending it deeper into the seabed.

This study emphasized that the critical stress ratio becomes more influential for deeper gouges in contrast to the shallower gouging depths; likewise, for denser soils compared to loose soils. Eskandari et al. concluded that the combination of the critical stress ratio and the state parameter has an evident influence on the seabed subgouge deformation rather than the effect of the critical stress ratio alone.

The authors used the analyses to propose an equation to estimate the horizontal reaction forces for the conditions studied.

4.3.9 Peek and Nobahar (2012)

In this study, Peek and Nobahar [41] used two types of models—coupled and uncoupled—to investigate the necessary burial depth of pipelines. In the uncoupled model, the soil was modeled by a set of nonlinear Winkler springs attached to the pipe at one end and displacement applied at the other end of the springs. In the coupled models, soil was treated as a 3D continuum medium and the ALE ABAQUS Explicit scheme was employed, which is similar to previous efforts of Nobahar (Nobahar et al., 2007 [38]). The value of this work lies in comparing the soil deformation and the pipeline response predicted by the two different approaches. Adding the subgouge deformations to the soil displacements, which were caused by the pipe load exerted on the soil, produced a superposition error. This error is apparently more influential than the coupling errors resulting from the directional coupling of Winkler springs in axial, lateral, and vertical directions.

4.4 Coupled Eulerian-Lagrangian

The CEL method attempts to capture the strength of the Lagrangian and the Eulerian methods. A Lagrangian mesh is used to discretize structures (in this case, the iceberg and the pipeline), while a Eulerian mesh is used to discretize the domain that is subjected to large deformations (in this case, the soil).

In the Eulerian formulation, coordinates of nodes are fixed and coincide with spatial points, but spatial coordinates of material points vary with time. There is no mesh distortion because the mesh is fixed in space (Figure 4.22). The material point at a given element quadrature point changes with time because the material flows through the mesh. This makes the definition of history-dependent materials difficult.

Boundary nodes and the material boundary may not coincide. Therefore, boundary conditions and interface conditions are difficult to apply.

In the Eulerian formulation (initially used in fluid mechanics), spatial coordinates are used to track the flow of the material in time through points fixed in space. As a result, large deformations can be easily simulated. Unfortunately, a fine mesh at the interface of Lagrangian and Eulerian domains is required to obtain high quality results. In addition, the Eulerian domain needs to be modeled to a larger extent so that no material leaves the specified domain.

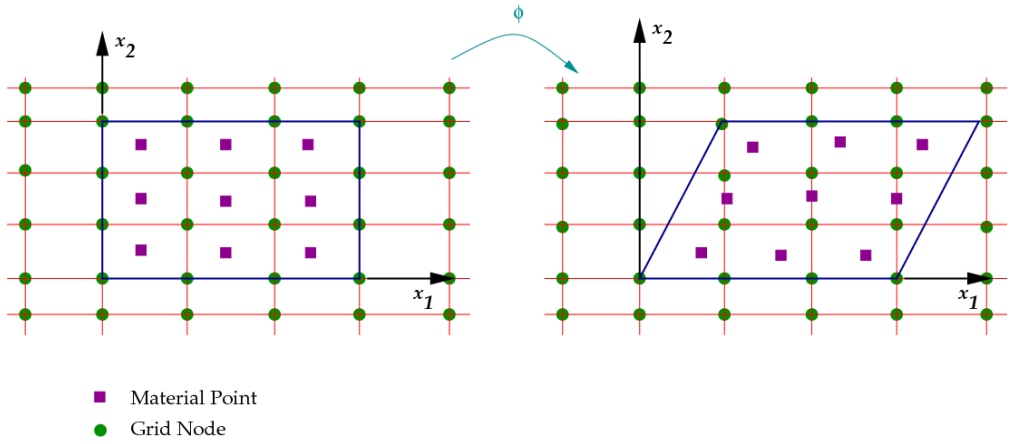

Figure 4.22: Eulerian Mesh Description

The interface between the structure (ice) and the soil is defined using the boundary of the Lagrangian domain. Interface models use the velocity of the Lagrangian boundary as a kinematic constraint in the Eulerian calculation, and the stress from the Eulerian cell is used to calculate the resulting surface stress on the Lagrangian domain.

4.4.1 Konuk and Gracie (2004)

Konuk and Gracie [24] presented numerical simulations that compare to the PRISE studies on subgouge deformations using LS-DYNA. The approach is referred to by the authors as Eulerian, but it is in fact similar to the Coupled Eulerian Lagrangian that is available in ABAQUS software, as the ice keel is a Lagrangian domain.

The results presented in this study indicate that the PRISE function may be overly conservative for the selected ice keel geometry, attack angle, and soil strength parameters. They also recognize the direct influence of these parameters on the magnitude and extent of subgouge deformations. Consequently, the authors suggested that future analysis should mimic the cases evaluated during the PRSE studies and should use parameters that are equivalent to those recorded in the experiments, including ice keel attack angle, geotechnical conditions (e.g., soil strength, effective stress path, drained/undrained loading), and interface friction.

Konuk and Gracie noted that although the Eulerian approach does not suffer from element distortion, numerical difficulties such as dissipation and dispersion problems associated with inter-element mass flux may be encountered. The work underlined the necessity of verification through comparison with centrifuge data and Lagrangian continuum FEA.

4.4.2 Jukes et al. (2008), Abdalla et al. (2009)

The models of Jukes et al. [21] [22] and Abdalla et al. [1] use the CEL formulation available in ABAQUS/Explicit software. The Eulerian domain labelled “VOID” in Figure 4.23 encloses all materials and the Lagrangian parts. It is divided into three parts: the initial seabed material, the initial trench backfill material, and the absence of material (or void). The pipeline extends outside the seabed and trench material, but it does not go beyond the Eulerian domain. The pipe was modeled as a three-dimensional, deformable, homogenous general-purpose shell. The ice indenter was modeled as a three-dimensional, solid, rigid shape Lagrangian part that moves through the Eulerian mesh.

The soil was modeled as a single-phase material, presenting undrained conditions using the modified Drucker-Prager/Cap constitutive model. The developed model was used to examine the effect of keel configurations (depth, width, attack angle). In this effort, the results from the developed CEL model, although limited to subgouge predictions in soft clay, were compared to selected PRISE centrifuge experimental data and the empirical PRISE function. The selected comparison data was obtained from the centrifuge testing performed by Lach (1996) [30], and the results were presented by two FE models: Konuk et al., 2005 [26] and Kenny et al., 2007 [29] (refer to Figure 4.24).

The soil parameters, gouge depth, gouge width, keel geometry, attack angles, and gouge speed were matched with Konuk’s 2005 model. Soil parameters used in the comparison study with Kenny et al. (2007) and the PRISE test were reasonably assumed because of the limited availability of the presented data.

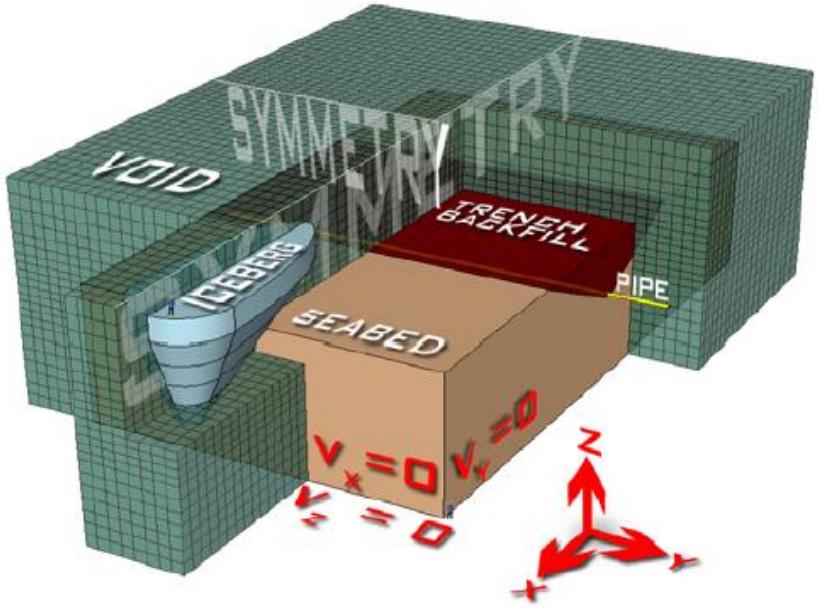

Figure 4.23: CEL Model Schematic (Abdalla et al., 2009 [1])

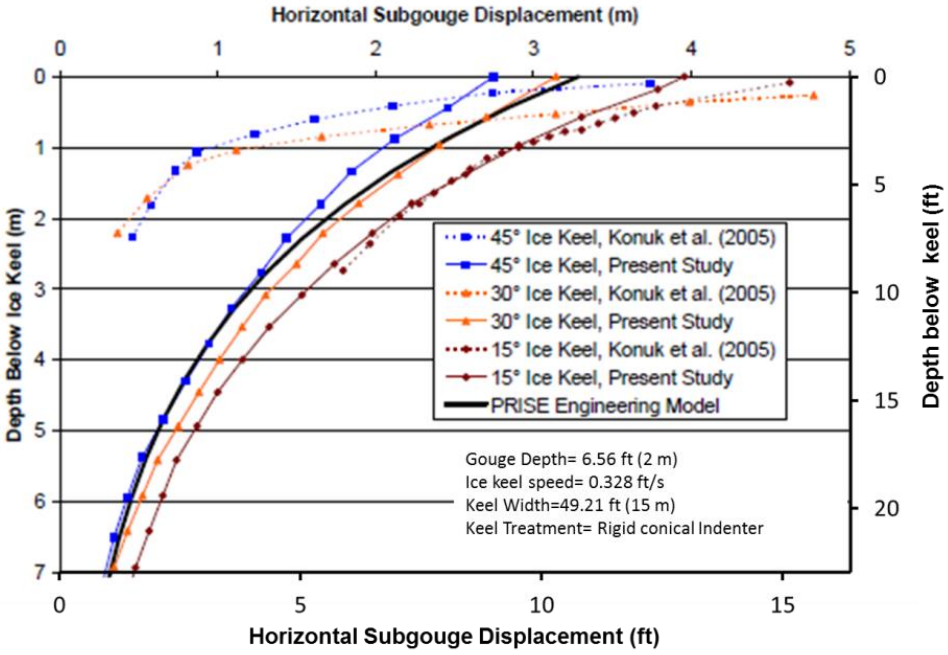

Figure 4.24: Comparison of Horizontal Subgouge Deformation Predictions with Konuk (Abdalla et al., 2009 [1])

The study concluded that for the same soil, deeper gouging keels produce larger subgouge soil deformations (Figure 4.25). This is consistent with the observations in the available literature.

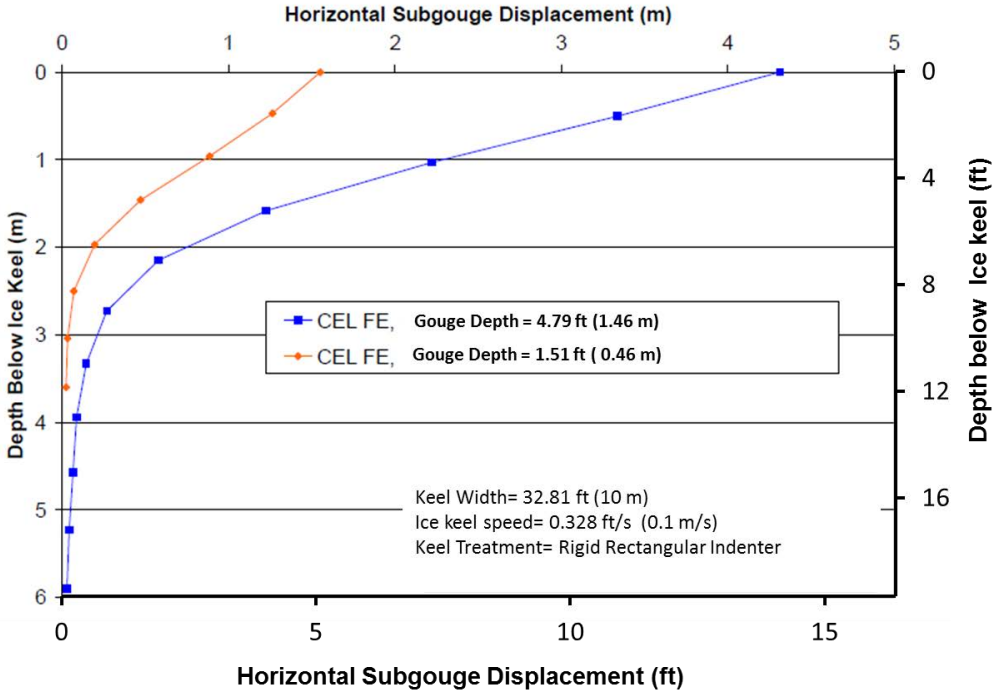

Figure 4.25: Effect of Gouge Depth on Subgouge Deformation (Abdalla et al., 2009 [1])

For shallow keel angles (15°), soil is compressed below the keel and then squeezed upwards, forming a low mound along the gouge sides. This side mound is higher in conical shape keels than in rectangular keels. On the other hand, for higher keel angles (30° and 45°), the soil is lifted upward ahead of the keel, forming a mound immediately in front of the keel, which subsequently clears to the gouge sides (Figure 4.26).

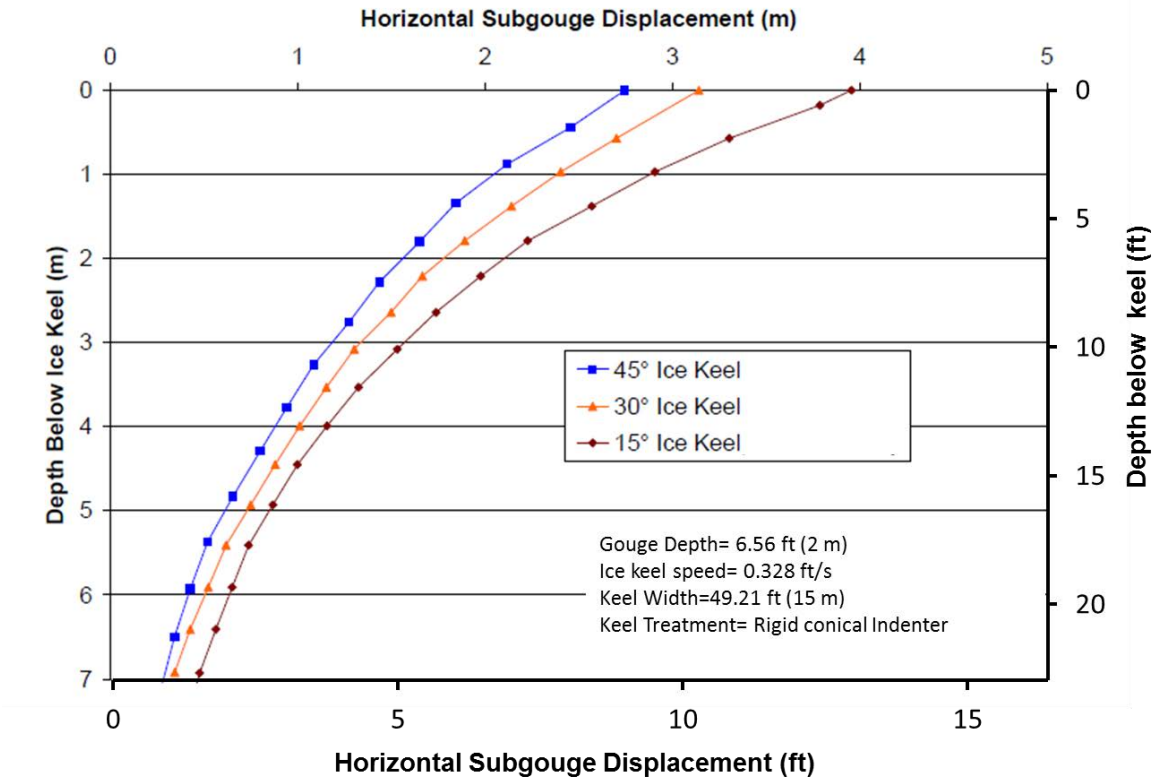

Figure 4.26: Effect of Keel Angle on Subgouge Deformation (Abdalla et al., 2009 [1])

Furthermore, the sharp edges of the rectangular keel produce higher stresses in the soil mass just beneath the keel-soil contact in comparison to the conical keel.

When compared to the PRISE data, the FE model predicted higher soil displacements immediately below the gouge base and within one to two gouge depths. The predicted soil displacements are smaller below this region. In general, the FE results generally agreed with the PRISE Engineering Model.

4.4.3 Phillips et al. (2010, 2011)

Phillips et al. [45] [46] presented a numerical ice-soil interaction model that was developed for sand with an emphasis on improving solution mesh dependency and sand constitutive behavior.

As part of the PIRAM JIP, a more realistic effective stress analysis was attempted using a Drucker-Prager cap variant with suppression of the dilatancy on the shear failure surface under high shear strains. The dilation angle varied with a user-defined subroutine between a minimum of 0° and a peak value of 11° to capture the effects of variable dilation.

The ice keel was generally modeled as a rough, inverted, truncated conical frustum of 49.2 ft. (15 m) minimum diameter (basal gouge width) and a 30° side slope, which was embedded to a gouge depth of 4.92 ft. (1.5 m). Sensitivity of the deformations and the keel reaction forces to mesh size were investigated by three levels of discretization (refer to Figure 4.27). A comparison of numerical results to the physical Subgouge Deformation (SGD) trend indicated that the mesh density refinement was adequate.

FEA results for gouging in saturated sand conditions were validated against the PRISE physical model data for similar conditions. Typical output visualization of FEA results is shown in Figure 4.28.

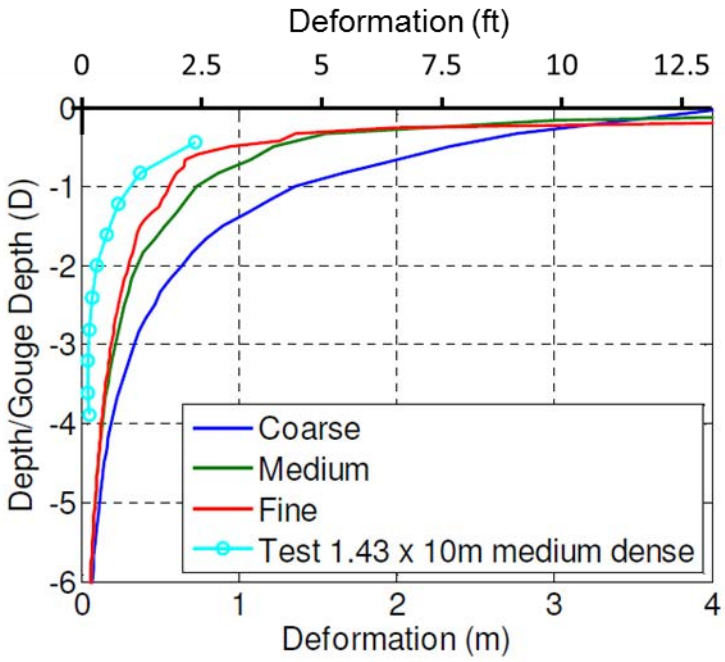

Figure 4.27: Subgouge Displacement Profiles (Phillips et al., 2011 [46])

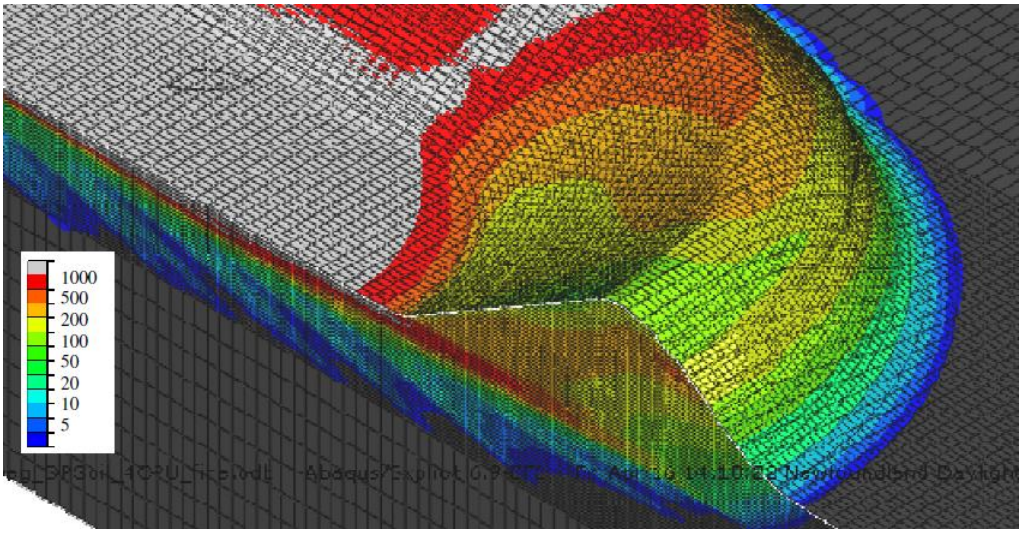

Figure 4.28: Percentage of Plastic Shear Strain Contours (Phillips et al., 2011 [46])

The keel reaction force varies significantly with the mesh size (Figure 4.29) and assumed dilational conditions (Figure 4.30).

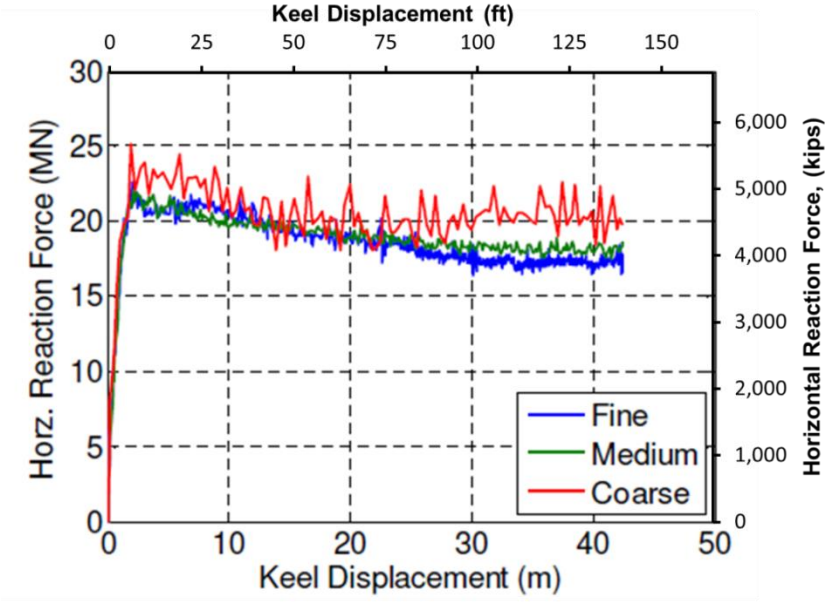

Figure 4.29: Keel Reaction Force Development with Varying Mesh Size (Phillips et al., 2011 [46])

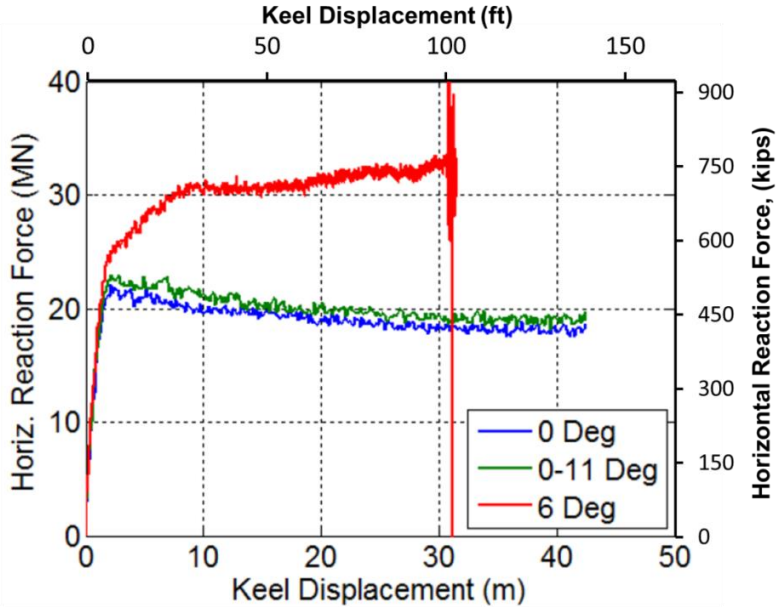

Figure 4.30: Keel Reaction Force with Varying Dilation (Phillips et al., 2011 [46])

Figure 4.31 shows how the variable dilation gives rise to a modest increase in SGD over the whole profile. The excessive plastic strains arising from the fixed dilation case (6°), give rise to excessive and unrealistic SGD shown by large plastic strains.

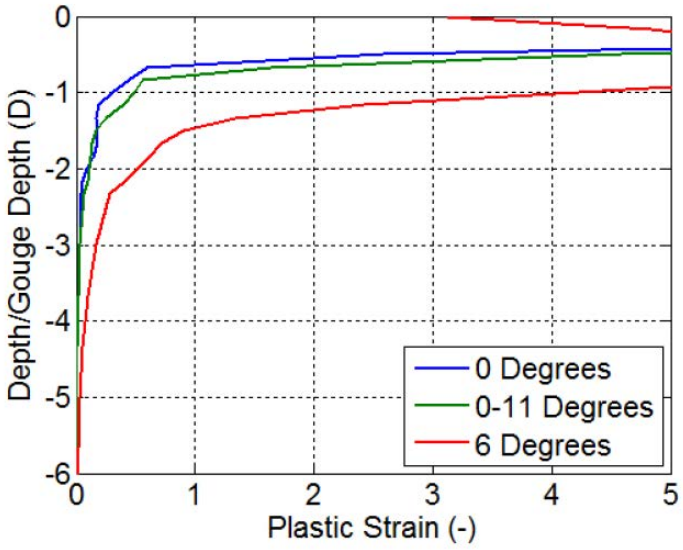

Figure 4.31: Plastic Strains Profiles Variation with Dilation (Phillips et al., 2011 [46])

The analyses emphasized the importance of dilation and stress level on the vertical extent and magnitude of subgouge displacements under gouges of differing scales. The soil constitutive models need to be improved to capture the appropriate effective stress behavior within a single-phase continuum.

4.4.4 Banneyake et al. (2011)

As contributors to the ice-pipe JIP, Banneyake et al. [3] conducted a series of ice gouging simulations where the effects of ice keel movement on the surrounding soil and on the pipeline were studied for a range of pre-specified modeling parameters. The simulations were preceded by a soil model calibration subtask with two selected PRISE tests: one for clay and another for sand. Figure 4.32 illustrates the Eulerian and Lagrangian components of the ice-soil-pipe CEL FEA model.

Comparisons of the numerically simulated triaxial compression tests and T-bar test results with the actual test data were used to verify the accuracy of the material model implementation. For the clay case, the simulated horizontal subgouge displacement results were comparable with those from the PRISE test, but the vertical subgouge displacements showed some disagreement. For the sand case, several discrepancies were observed between the simulation and the test results, possibly because of a lack of details in the sand parameters used in the PRISE tests.

Increases in the gouge depth, keel attack angle, and keel width caused increases in the height of the side berms and frontal mounds (Figure 4.33). Side berms in sandy seabeds were higher than those in clayey seabeds (Figure 4.34). Larger keel angles resulted in a scraping-like removal of the soil, which reduced the subgouge soil deformation and hence the pipe displacement.

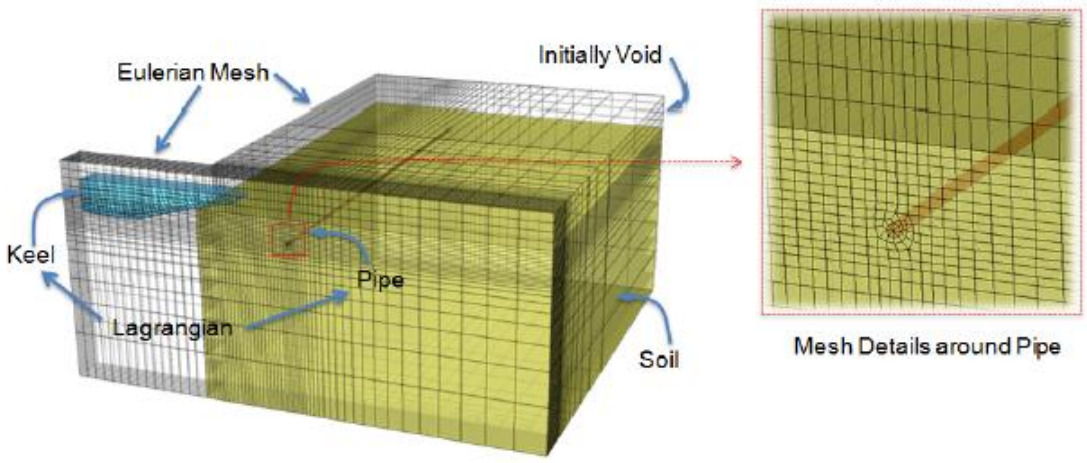

Figure 4.32: Eulerian and Lagrangian Components of the Ice-Soil-pipe CEL Model (Banneyake et al., 2011 [3])

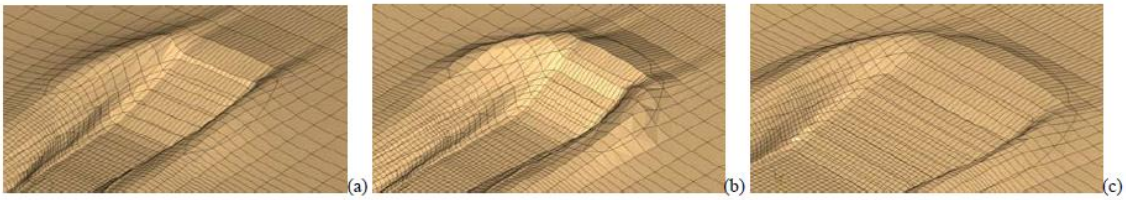

Figure 4.33: Effect of Keel Size and Angle (DOG-11.5 ft.) (a) Width=32.8 ft. and Angle 15°, (b) Width=32.8 ft. and Angle 30°, (c) Width=98.5 ft. and Angle 15° (Banneyake et al., 2011 [3])

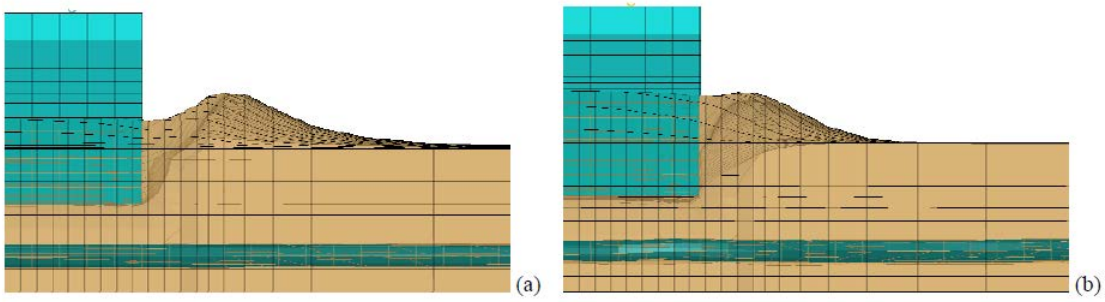

Figure 4.34: Side Berm Formation in Clayey (a) and Sandy (b) Seabed (Banneyake et al., 2011 [3])

Sandy seabeds resulted in subgouge deformation and pipe curvature that were greater than those observed in the clayey seabed. The decrease in pipe diameter showed detrimental effects on the pipe deformation, as was anticipated. Soil movement in the upper soil zone remained similar for the two pipe diameters. However, the soil around the pipe showed a significantly higher range of motion when the pipe diameter was reduced. A change in pipeline stiffness affects the extent of pipe deformation under soil pressure and the resistance offered to soil deformation by the pipe.

The lateral subgouge soil movement in sand had a very high gradient in the vertically upward direction compared to that in clay. Therefore, the pipeline's lateral deformation appeared to be higher in the normally consolidated sand than in the medium dense clay model. The sand experienced more of the scraping-like removal by the keel and was less susceptible to squeezing into side berms. Hence, pipe in a sandy seabed does not demonstrate the level of lifting that is observed in clayey seabeds.

4.4.5 Lele et al. (2011)

Lele et al. [33] developed a CEL model to evaluate its capability to characterize the ice gouging process and to accurately estimate pipeline strain demand. Soil was modeled using a Eulerian mesh, while the pipe and rigid ice keel were modeled in the Lagrangian domain. An illustration of the model is shown in Figure 4.35, and the mesh refinement details can be seen in Figure 4.36.

The authors used the von Mises elastic-plastic material model for modeling clay and the Drucker-Prager model for sand. They noted that software in-built Drucker-Prager models (with and without the cap) may lead to unrealistic excessive dilation in large deformation analysis, especially when using finer meshes. The authors implemented a user subroutine in this study, and it prevented this excessive dilation.

Lele et al. conducted a limited parametric study to determine the effect of gouge depth, gouge width, pipe diameter, and pipe wall thickness on pipeline strain demand. The authors also assessed the effect of pipe burial depth for a constant gouge depth.

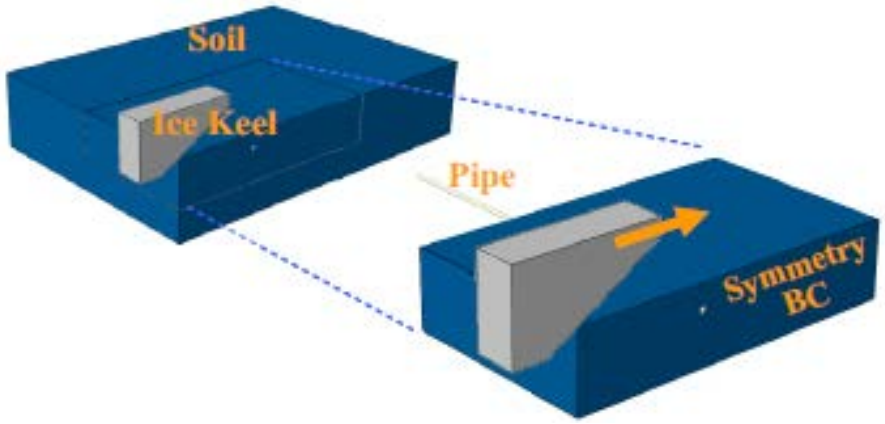

Figure 4.35: Finite Element Model (Lele et al., 2011 [33])

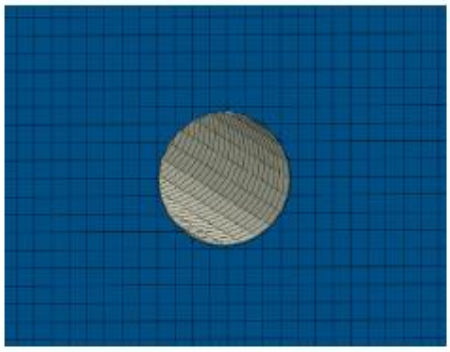

Figure 4.36: Mesh Refinement in the Pipe-Soil Contact Region (Lele et al., 2011 [33])

A comparison of the results produced by this study and the PRISE experiment is shown in Figure 4.37.

Lele et al. were confident that learnings from the continuum approach results could be used to improve the accuracy of soil-spring based models so as to avoid the cost of continuum model parametric studies in the conceptual design phase.

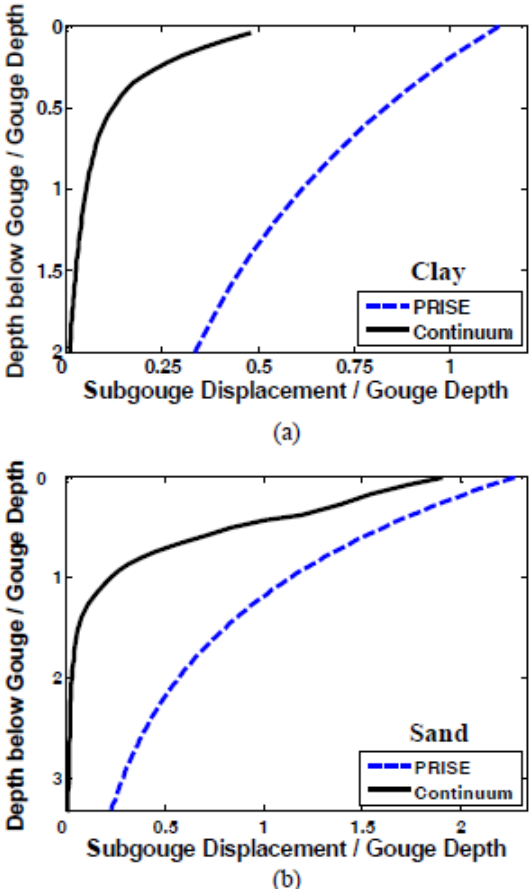

Figure 4.37: Comparison of Subgouge Soil Deformation Predicted by Continuum Model and PRISE Equation: (a) Clay (b) Sand (Lele et al., 2011 [33])

4.4.6 Panico et al. (2012)

The work of Panico et al. [40] extended the scope of Lele et al., 2011 [33] and investigated the effect of the frictional properties of sand on gouge forces and subgouge displacements by implementing two sand friction models. The two friction models—one with constant friction and the other with varying friction—are shown in Figure 4.38. The authors concluded that, in sand, ice gouging response is mainly controlled by critical state behavior with the peak friction angle having a limited effect on gouge force and subgouge displacements (refer to Figure 4.39).

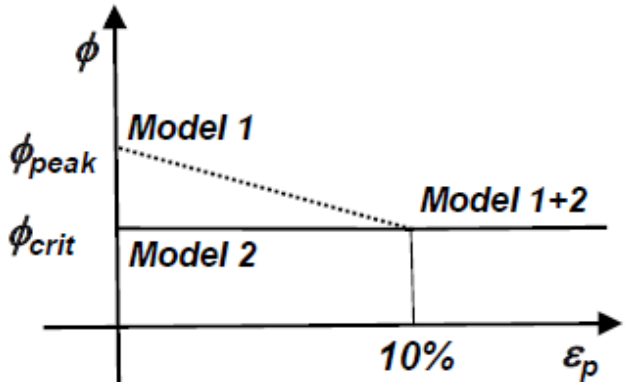

Figure 4.38: Dependence of Sand Friction Angle on Equivalent Plastic Strain for Model 1 and Model 2 (Panico et al., 2012 [40])

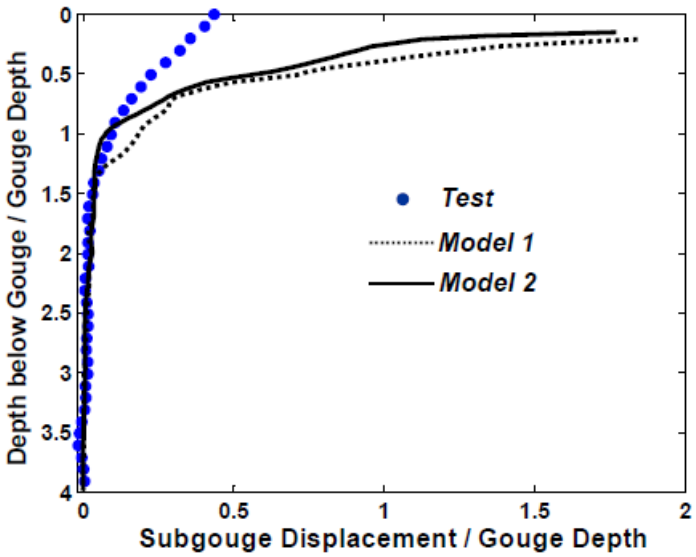

Figure 4.39: Comparison of Subgouge Displacement Profile for Model 1 and 2 with Centrifuge Experiment (Panico et al., 2012 [40])

A comparison between centrifuge tests showed that the continuum model can reasonably estimate gouge forces with a maximum error in the order of 30%, which is considered reasonable, given the level of uncertainties associated with the characterization of sand properties and the preparation of a uniform test bed in centrifuge experiments.

The comparison conducted between centrifuge tests, the continuum approach, and the soil-spring approach for both a thick- and thin-walled pipe scenario showed that continuum models can adequately predict the pipe strain demand (see Figure 4.40). In both cases, the soil-spring approach predicted much larger pipe strains than the continuum approach.

The Panico study showed some preliminary validation of the continuum approach using small-scale centrifuge tests, but full validation requires a comparison of ice gouging continuum models with large-scale test data, which are currently limited. When full validation is completed, the authors are confident that continuum models can be effectively used to improve the reliability and cost effectiveness of the design.

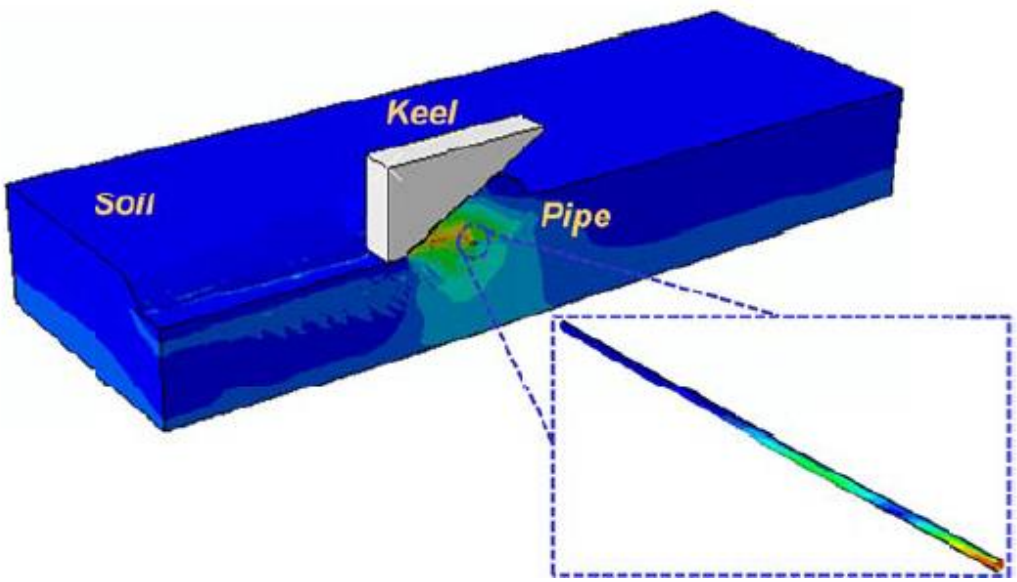

Figure 4.40: Continuum Simulation of Ice Gouging Process and Induced Strains on Pipeline (Panico et al., 2012 [40])

4.4.7 Rossiter and Kenny (2012)

Rossiter and Kenny [48] conducted a parametric study to examine the influence of attack angle and interface properties on soil behavior and pipeline mechanical response. Table 4.1 summarizes the cases studied by the researchers. The initial intention was to use the CEL formulation because of its robust modeling capabilities. However, the authors identified technical issues related to interface shear strength behavior and contact mechanics within the ABAQUS/CEL modeling framework. This work used ALE formulations in LS-DYNA to simulate both free field and coupled ice gouge events.

Table 4.1: Cases Examined in the Study (Rossiter and Kenny, 2012 [48])

Cases	Keel Attack Angle (degrees)	Ratio	(ft.)
Case 5	15	5	24.61
Case 6	15	10	49.21
Case 7	15	15	73.82
Case 8	15	20	98.43
Case 9	30	10	24.61
Case 10	30	10	49.21

From analysis of the contact stress developed at the ice keel/seabed interface, the authors observed that the interface frictional forces did not correctly account for the equivalent shear stress limit (τ_{max}). The shear stresses developed to a value that was much lower than the defined τ_{max}, which resulted in greater clearing and subduction of the soil, causing incorrect estimation of the seabed reaction forces. The analysis illustrated that weaker interface properties allow for greater subduction below the keel and therefore result in less material buildup in front of the keel.

Horizontal to vertical force ratios were within the range of the centrifuge data of Lach (1996) [30] and PRISE (Figure 4.41). Plots of horizontal subgouge deformations revealed an increase in deformation with an increase in keel width. However, there is a potential trend in the data that suggests a limiting keel width, as the model tends to a plane strain-type condition.

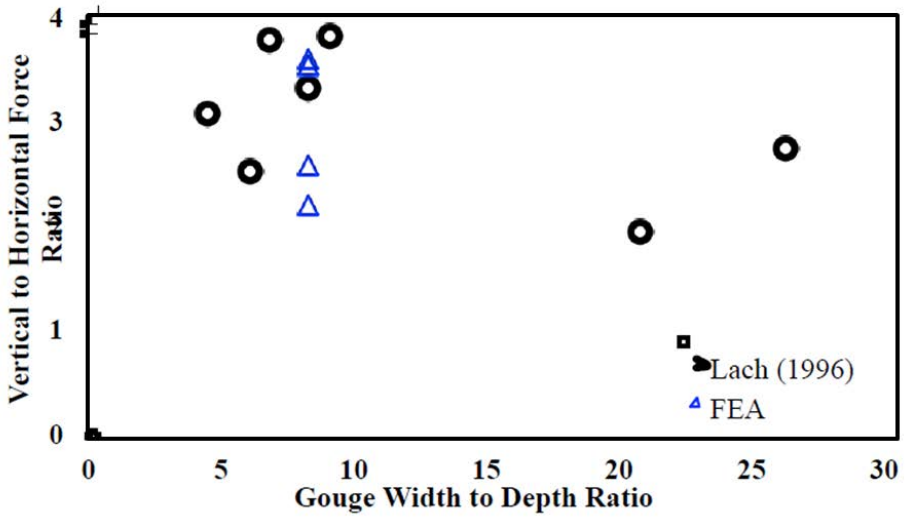

Figure 4.41: Comparison of Results with Lach's Experimental Data (Rossiter and Kenny, 2012 [48])

For the ice keel attack angles investigated (results shown in Figure 4.42), the side berm elevations were not as sensitive to changes in Su and τ_{max} with only slightly decreasing trends for decreasing values of these properties. These results suggest that higher strength soils have higher frontal mound elevation and less material being cleared to the side berms, while weaker soils have less resistance to subduction and clearing mechanisms and therefore have less material developing in front of the gouging keel.

The Rossiter and Kenny paper illustrates the importance of soil representation and interface conditions on the soil response. ABAQUS CEL numerical models that have being partially calibrated with reduced-scale centrifuge data may not produce realistic results (outside the calibration domain) with respect to clearing mechanisms, interface conditions, and contact mechanics. This perspective introduces a significant uncertainty when examining free field or fully coupled ice gouge events outside the calibration dataset conditions.

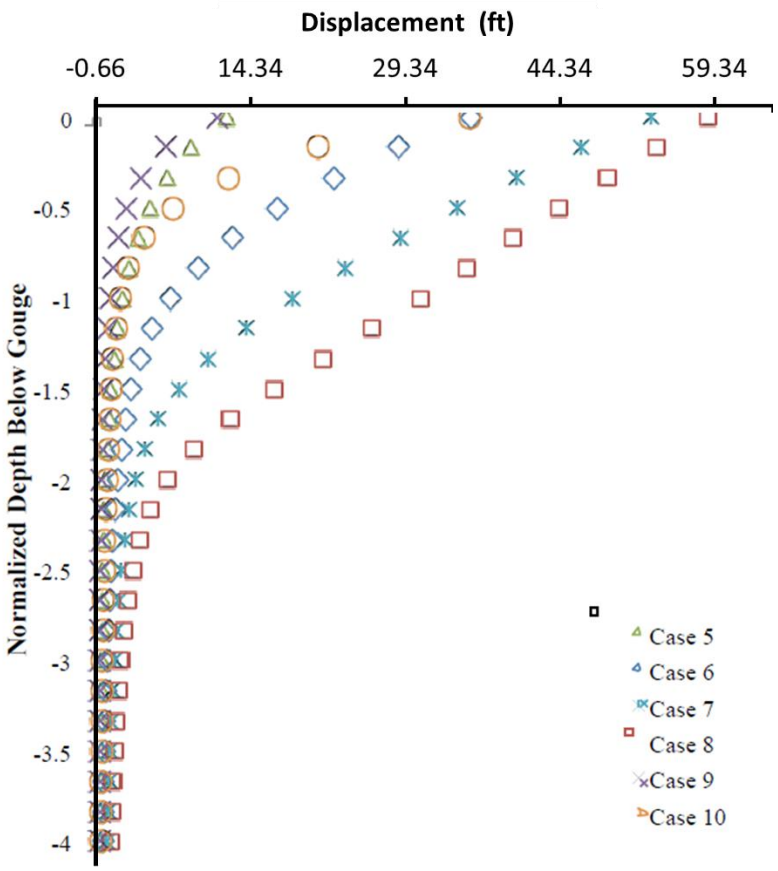

Figure 4.42: Horizontal Subgouge Deformation for Varying Gouge Widths and Keel Attack Angles (Rossiter and Kenny, 2012 [48])

4.4.8 Pike and Kenny (2012)

Pike and Kenny [42] developed a prototype numerical model of Lach's centrifuge test in clay. Lach, 1996 [30] provided the model details, variability of undrained shear strength with depth (Su), variation of overconsolidation ratio (OCR), and common Speswhite kaolin index properties.

Horizontal and vertical keel reaction forces and subgouge soil displacements were in good agreement with the physical dataset as well as the numerical predictions of horizontal subgouge soil deformations by a semi-empirical equation derived from centrifuge tests in clay (Woodworth-Lynas et al., 1996 [56]), commonly referred to as the PRISE equation.

The agreement between the numerical and centrifuge test data tends to diverge in the upper 3.28 ft. (1 m) beneath the base of the gouge. This is explained by a shift from a continuum mechanical response to a localized zone of high shear that is difficult to

capture with the current mesh resolution. Furthermore, the element formulation is such that the strain is constant within each element, thus making it difficult to capture sharp strain gradients. The authors showed that when assessing the effect of ice keel shape on subgouge soil deformation, steep keels produce less severe subgouge deformations.

The study showed the variability of soil strength profiles in the Canadian Beaufort for the Amauligak F24 and Tarsuit P45 sites as provided by Crooks et al. 2007 [11] and Rogers et al. 1993 [47]. The shear strength profiles in these two locations are presented in Figure 4.43. As expected, the soil strength profile has a profound effect on subgouge deformation fields (refer to Figure 4.44).

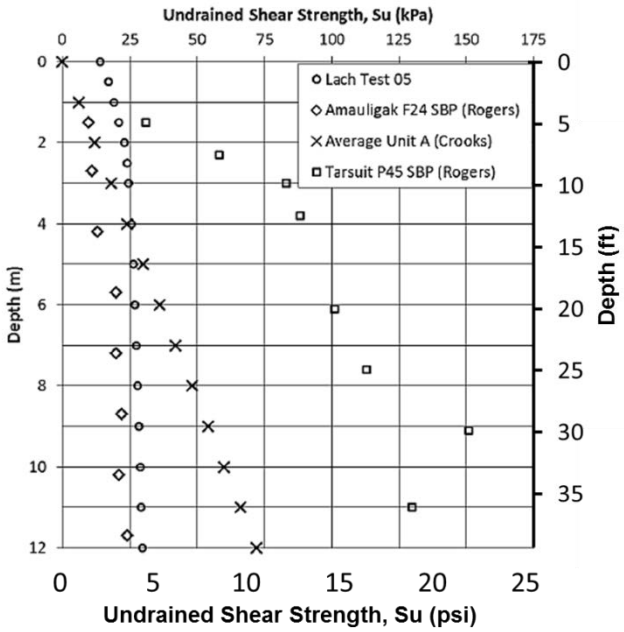

Figure 4.43: Undrained Shear Strength Profiles of Some Beaufort Sea Clays (Pike and Kenny et al., 2012 [42])

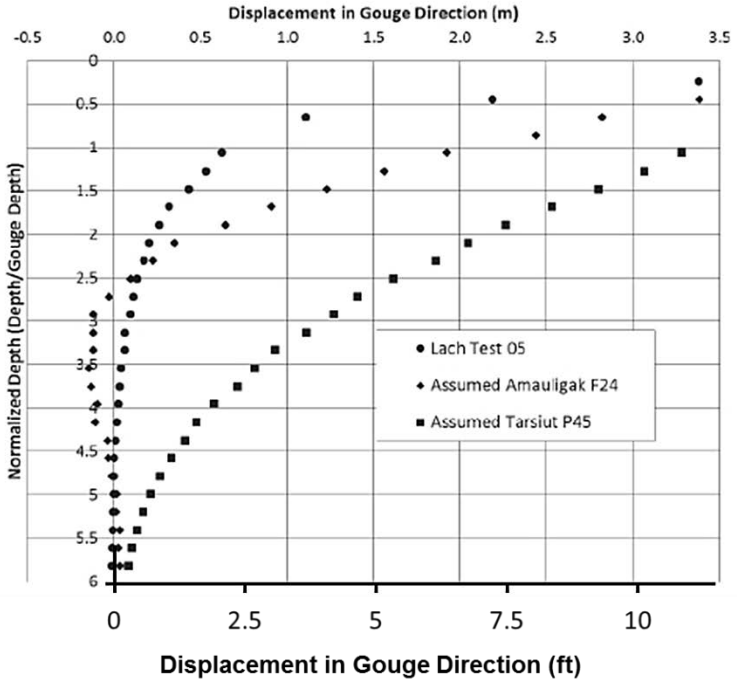

Figure 4.44: Effect of Varying Soil Strength Profiles on Horizontal Subgouge Deformations (Pike and Kenny et al., 2012 [42])

4.4.9 King et al. (2012)

King et al. [23] developed a 3D seabed model with a rectangular sub-surface caisson using ABAQUS FE modeling and a CEL scheme. The intention was to assess the feasibility of such structures as an alternative to placing them inside an Excavated Drilling Center (EDC), based on the conditions encountered on the Grand Banks in offshore Newfoundland, Canada.

The authors considered a scenario of an ice keel scouring over a buried caisson, avoiding direct contact but with minimal clearance (refer to Figure 4.45 and Figure 4.46). A centrifuge testing program, consisting of five tests, formed the basis for the calibration of an FE model. The results indicated that the proposed numerical model performed satisfactorily when simulating the centrifuge tests and that a caisson system can potentially provide the protection needed for subsea installations. Based on the authors' recommendation, future work should involve evaluating various ice keel-soil-structure interaction scenarios and attack angles as well as assessing in detail the construction and installation issues of such work.

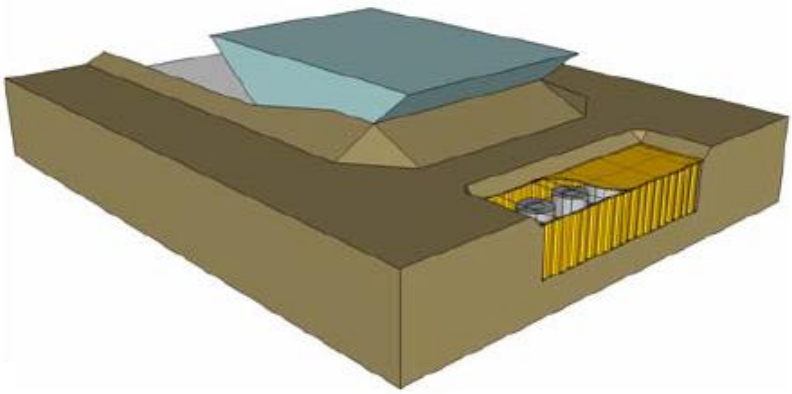

Figure 4.45: Illustration of Protection Caisson and Keel-Soil Interaction (King et al. 2012 [23])

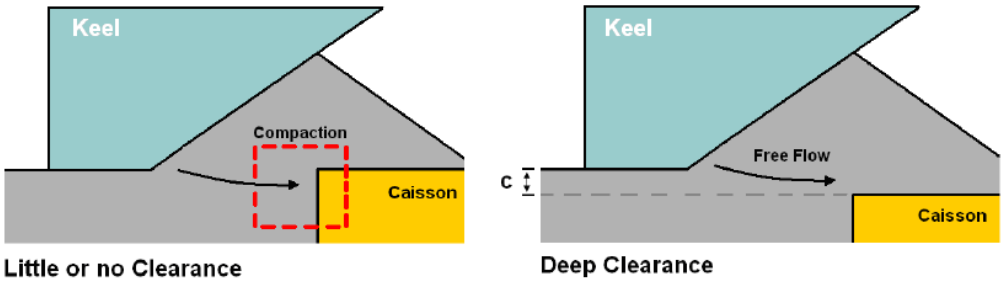

Figure 4.46: Numerical FE Analysis on the Influence of Clearance on Soil Forces Experienced by the Caisson (King et al. 2012 [23])

Figure 4.47 illustrates the effect of keel roughness to the envelope of induced displacements. The roughness of the keel affects the magnitude of the displacements experienced by the soil mass in the frontal mount.

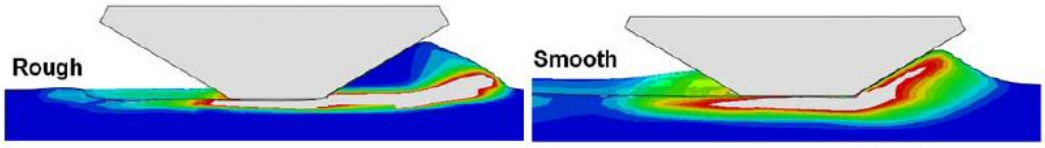

Figure 4.47: Numerical FE Analysis on the Effect of Keel Roughness on Soil Displacement (King et al. 2012 [23])

4.5 Smoothed Particle Hydrodynamics

The advantage of the mesh-free methods is that nodes and elements are not defined; instead, only a collection of points is necessary to represent a given body. Wu et al. [57] first used a mesh-free method in 2001 to study geotechnical materials. However, mesh-free methods have not been popular because commercial software producers have not yet widely adopted their use. Another reason is that assessing nodal interactions without an explicit mesh appears to make mesh-free methods computationally expensive.

Smoothed Particle Hydrodynamics (SPH) is a numerical method that is part of the larger family of mesh-less (or mesh-free) methods. The coordinates move with the fluid, and the resolution of the method can be easily adjusted with respect to the variables (e.g., density). The SPH method works by dividing the fluid into a set of discrete elements, referred to as particles or pseudo-particles. These particles have a spatial distance (known as 'smoothing length') over which their properties are 'smoothed' by a kernel function. This means that the physical quantity of any particle can be obtained by summing up the relevant properties of all the particles that lie within the range of the kernel.

SPH is based on a fully Lagrangian modeling scheme. This fact permits the discretization of a prescribed set of continuum equations by interpolating the properties directly at a discrete set of points distributed over the solution domain without the need to define a spatial mesh. The method's Lagrangian nature combined with the absence of a fixed mesh is its main strength.

As discussed by Pike et al. (2012) [42], ABAQUS-Simulia representatives have noted that the SPH method is less accurate than the CEL method in higher deformation regimes. Pike et al. also notes that if a large percentage of all nodes in the model are associated with SPH, the analysis may not scale well if multiple Central Processing Units (CPUs) are used. Because there is currently no capability for automatically computing the volume associated with these particles, it is necessary to distribute the particle elements uniformly. Therefore, bias meshing in elastic regions of the problem domain to reduce the number of particles is not currently an option. This, combined with poor parallel scalability and the need for small particle spacing to capture strain localization, may make this method less effective for the extension of structure/soil interaction problems to coupled ice keel/soil/structure interaction scenarios.

4.5.1 Fredj et al. (2010)

The Fredj et al. [17] study does not refer directly to an ice gouge event, but it does describe the application of a 3D continuum modeling technique for assessing the performance of a pipeline system that is subjected to large soil displacements. This analytic process made use of LS-DYNA SPH modeling capability and considered a wide range of soil types and soil movement scenarios. The authors compared the results with published experimental data of large-scale tests to verify the numerical analysis method. The authors noted that the test data came from a large-scale tank experiment investigating pipe-soil load transfer caused by large lateral soil movements and not an ice gouge event. A comparison between numerical predictions and full-scale experiment results showed a good agreement, indicating that the SPH method can satisfactorily simulate the observed pipeline response and soil deformation in certain pipe-soil interaction scenarios.

4.6 Other Continuum Methods

The Particle-In-Cell (PIC) model is based on the ideas of approximating saturated soil as an incompressible viscous fluid and generalizing the formulation to soil-structure/object interaction in a large deformation framework. Within this approach, the soil-ridge and soil-pipe interactions are treated as fluid-object and fluid-structure interaction problems, respectively. The arbitrarily large topological changes in the soil are accommodated by representing the water-soil interface as a single dynamic implicit surface.

4.6.1 Sayed and Timco (2009)

Sayed and Timco's paper [49] presents an alternative approach for the numerical modeling of the soil gouging process by treating the soil as a highly viscous non-Newtonian fluid, thereby converting the deformation to viscous flow. Deformation of the seabed material was considered to be elastic-plastic and followed a Mohr–Coulomb criterion. Compressibility was introduced through a pressure–solids volume fraction relationship. The numerical scheme employed a PIC advection method, where the soil was represented by discrete particles, making it possible to handle discontinuities and large deformations. Numerical analyses considered 2D deformation of seabed soil against a vertical moving indenter, representing an iceberg keel. The authors simulated a buoyant iceberg and compared the results with experimental data. The resulting deformation patterns were similar to the slip (shear) planes that are considered in plastic limit analyses (e.g., Schoonbeek et al., 2006 [50]). The authors further noted that displacements took place mostly in wedges that formed in front of the rigid indenter, near the free surface. Vertical profiles of the velocities and normal stresses (Figure 4.48) provided quantitative measures of the disturbance of the soil beneath the scour depth.

The simulation showed that stresses in front of the iceberg are higher than the values corresponding to passive earth pressure because of the inertia of the moving soil. The resulting deformation patterns, which are shown in Figure 4.49, display failure zones and the development of shear zones as described by other researchers (e.g., Schoonbeek et al., 2006 [50]). The simulations examined the dependence of stresses on scour depth, soil properties, compaction, and scour velocity and were compared with experimental data. The results show that the mean normal stress on the iceberg increased with deeper scours and higher angles of internal friction in sands.

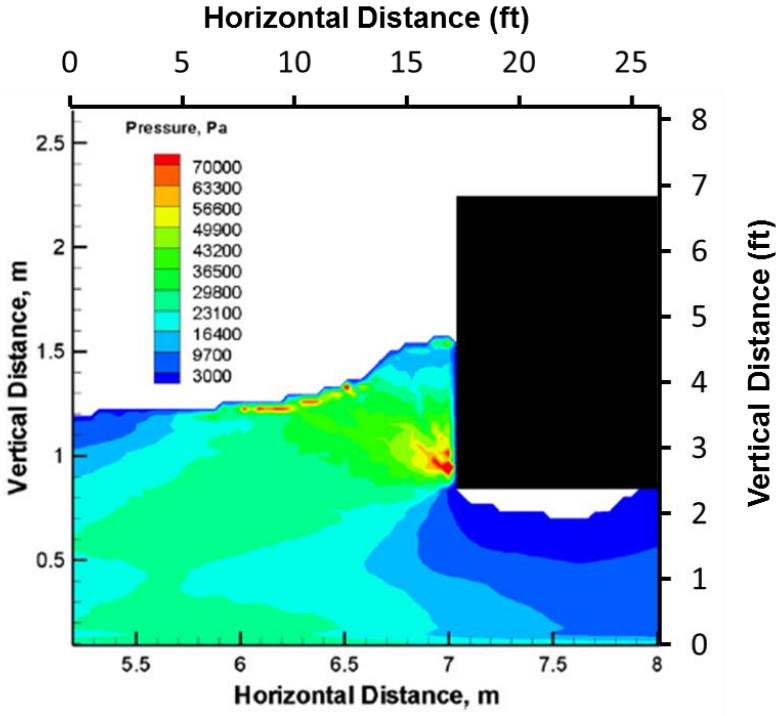

Figure 4.48: Contour Plot of the Pressure for the Reference Case (Sayed and Timco, 2009 [49])

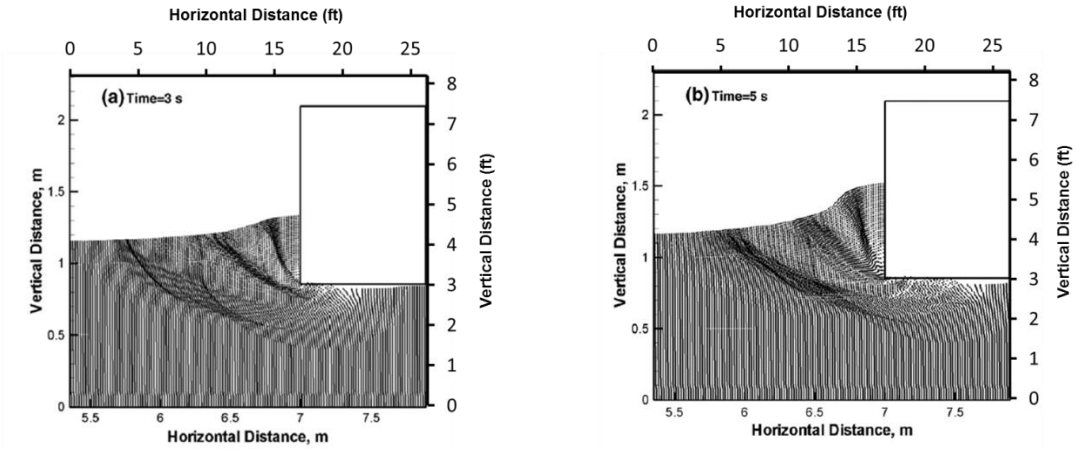

Figure 4.49: Snapshots of Particle Positions (a) 3 sec. After the Start of the Simulation (b) 5 sec. After the Start of the Simulation for the Reference Case (Sayed and Timco, 2009 [49])

5.0 Findings/Recommendations

The numerical simulations of ice gouging have evolved over the years. Currently, simulations are more sophisticated and complex, and they require increased computational power. However, there is still room for improvement in the following areas:

1. Uncertainty of Input Parameters

Repetitive surveys of gouge events and data from iceberg tracking efforts in different areas cannot confidently establish correlations between geometric variables or other important physical parameters such as water depth, ice features (e.g., type and strength), gouge depth and width, gouge rate, and soil type.

Knowledge of the geometric properties of the ice keel (including ice keel width, depth, attack angle, and spatial variation of these parameters within the ice feature) are vital for improving simulation efficiency and evaluating the performance of subsea structures against realistic ice gouging scenarios.

In addition, the uncertainty of local site conditions (stratigraphy and soil profile) and soil parameters (e.g., strength, density) are additional challenges for simulating actual ice gouge processes. These issues are significant for non-cohesive material (e.g., sand) where a greater degree of uncertainty exists when compared with cohesive material (e.g., clay).

2. Computational Tool Capabilities

Advancements in the software package capabilities are required to incorporate:

a. Two-phase material within an effective stress analysis to account for the effects of pore pressure and associated volumetric changes caused by plastic shear strain (e.g., modified Cam-Clay plasticity model).
b. Improvements of constitutive models for ice and soil (e.g., effective stress analysis, nonlinear subyield behavior, strain softening/hardening response) through calibration of the numerical procedures to physical experimental and laboratory testing data.

3. Validation of Results

So far, numerical models have been calibrated using results from small-scale testing. Currently, the availability of large-scale data to validate numerical models is extremely limited because of the high cost and uncertainty associated with this type of testing methodology. When full validation is completed, continuum models can be effectively used to improve the reliability and cost effectiveness of the design of subsea structures subjected to ice gouging hazards such as pipelines and wellheads.

A comprehensive review of the available literature identified the scarcity of numerical models that included wellheads. This is an important gap that should be bridged with further numerical efforts.

6.0 References

1. Abdalla, B., Pike, K., Eltaher, A., Jukes, P., and Duron, B. (2009). "Development and Validation of a Coupled Eulerian Lagrangian Finite Element Ice Scour Model." 28th International Conference on Ocean, Offshore and Arctic Engineering, OMAE2009, pp. 87-95.
2. ASCE, 1984. "Guidelines for the Seismic Design of Oil and Gas Pipeline Systems." Committee on and Liquid Fuel Lifelines, Technical Council on Lifeline Earthquake Engineering.
3. Banneyake, R., Hossain, M.K., Eltaher, A., Nguyen, T. and Jukes, P. (2011). "Ice-Soil-Pipeline Interactions Using Coupled Eulerian-Lagrangian (CEL) Ice Gouge Simulation- Extracts from Ice Pipe JIP." Arctic Technology Conf., Houston, TX, USA.
4. Been, K., Kosar, K., Hachey, J., Rogers, B.T., and Palmer, A.C. (1990). "Ice Scour Models." Proc., OMAE, Vol. 5, pp.179-188.
5. C-CORE (1993). Pressure Ridge Ice Scour Experiment (PRISE) Phase 2: Progress Report. C-CORE Report 93-C4, March, 105p.
6. C-CORE (1995). Pressure Ridge Ice Scour Experiment (PRISE) Phase 3: Engineering Model Application. C-CORE Report 95-C12, August.
7. C-CORE (1997). Pressure Ridge Ice Scour Experiment (PRISE) Phase 3C: Extreme Ice Scour Event – Modeling and Interpretation, Review and Development of Finite Element Modeling. C-CORE Report 97-C20, April, 27p.
8. C-CORE (1998). "Safety and Integrity of Arctic Marine Pipelines. Report for the Minerals Management Service." C-CORE Report 98-C15, June, 41p.
9. C-CORE (2000). "Risk Assessment of Ice Damage to Buried Marine Pipelines." C-CORE Report 00-C31, October, 192p.
10. Committee on Gas and Liquid Fuel Lifelines. (1984). "Guidelines for the Seismic Design of Oil and Gas Pipeline System." Technical Council on Lifeline Earthquake Engineering, ASCE, New York.
11. Crooks, J., Been, K., Becker, D., and Jefferies, M. (2007). "Geology, Characterization and Properties of Beaufort Sea Clays." In Characterization and Engineering Properties of Natural Soils. Taylor & Francis. doi:10.1201/NOE0415426916.ch7
12. Donea, J., Huerta, A., Ponthot, J.-Ph., and Rodrıguez-Ferran, A. (2004). "Arbitrary Lagrangian–Eulerian Methods." Encyclopedia of Computational Mechanics, Erwin Stein, René de Borst and Thomas J.R. Hughes Editors. Volume 1: Fundamentals. John Wiley & Sons.
13. Eskandari, F., Phillips, R., and Hawlader, B. (2010). "A State Parameter Modified Drucker-Prager Cap Model." Canadian Geotechnical Conference.

14. Eskandari, F., Phillips R., and Hawlader, B. (2011) "Ice Gouging Analysis Using NorSand Critical State Soil Model." 2011 Pan-Am CGS Geotechnical Conference, paper# 995
15. Eskandari, F., Phillips R., and Hawlader, B. (2012) “Finite Element Analyses of Seabed Response to Ice Keel Gouging,” Proc. 65th Canadian Geotechnical Conference Winnipeg, Manitoba, 2012.
16. Fredj, A., Comfort, G., and Dinovitzer, A. (2008). “A Case Study of High Pressure/High Temperature Pipeline for Ice Scour Design Using 3D Continuum Modeling.” In ASME 2008 27th International Conference on Offshore Mechanics and Arctic Engineering (pp. 563-572). American Society of Mechanical Engineers.
17. Fredj, A. and Dinovitzer, A. 2010. Three-dimensional Response of Buried Pipeline Subjected to Large Soil Deformation Effects – Part I: 3D Continuum Modeling Using ALE and SPH formulations, 8th Int. Pipeline Conf., Calgary, Alberta, Canada.
18. Jefferies, M. G., and Been, K. (2006). Soil Liquefaction: A Critical State Approach, Taylor & Francis.
19. Jordaan, I. J. (2001). “Mechanics of Ice-Structure Interaction.” Eng. Fract. Mech., 6817–18, 1923–1960.]
20. Jukes, P., Eltaher, A., Abdalla, B., and Duron, B. (2008). “The Design and Simulation of Arctic Subsea Pipelines.” DNV Conference on Arctic activities, Høvik.
21. Jukes, P., Eltaher, A., Abdalla, B., and Duron, B. (2008). “The Design and Simulation of Arctic Subsea Pipelines.” Russia Offshore, 3rd Annual Meeting, Moscow.
22. Jukes, P., Eltaher, A., Abdalla, B., and Duron, B. (2008). “The Design and Simulation of Arctic Subsea Pipelines—Ice Gouging Formulations.” 4th annual Arctic Oil & Gas Conference, Oslo, Norway.
23. King, T., Ralph, F., Barrett, J., and Zakeri, A. (2012). “Physical and Numerical Modeling of a Sub-Surface Caisson for Protection of Subsea Facilities Against Scouring Icebergs.” Offshore Technology Conference. doi:10.4043/23789-MS
24. Konuk, I. and Gracie, R. (2004). A 3-dimensional Eulerian Finite Element Model for Ice Scour. Proceedings of IPC 2004, Calgary, AB. Paper IPC04-0075.
25. Konuk, I.S., Fredj, A. (2004b). “An FEM Model for Pipeline Analysis of Ice Scour.” Proc., OMAE, OMAE2004-51477.
26. Konuk, I.S., Yu, S., and Gracie, R. (2005). “An ALE FEM Model of Ice Scour.” Proc., IACMAG, Vol.3, pp.63-70.
27. Kenny, S., Bruce, J., King, T., McKenna, R., Nobahar, A., and Phillips, R. (2004). “Probabilistic Design Methodology to Mitigate Ice Gouge Hazards for Offshore Pipelines.” Proc., IPC, IPC04 0527, 9p.

28. Kenny, S., Nobahar, A., Phillips, R., and Clark, J.I. (2005). “PRISE Studies on Subgouge Deformations and Pipeline/Soil Interaction Analysis.” Proc. 18th. Int. Conf. POAC.
29. Kenny S., Barrett J., Phillips R., and Popescu, R. (2007). Proceedings of the Seventeenth 2007 International Offshore and Polar Engineering Conference, ISOPE 2007.
30. Lach, P.R. (1996). “Centrifuge Modeling of Large Soil Deformation Due to Ice Scour.” Ph.D. Thesis. Memorial University of Newfoundland, St. John's, Newfoundland, 685p.
31. Lach, R.R. and Clark, J.K. (1996). “Numerical Simulation of Large Soil Deformation Due to Ice Scour.” The 49th Canadian Geotechnical Conference of the Canadian Geotechnical Society, Vol.1 pp. 189-198.
32. Lach, R.R., Clark, J.K., and Poorooshasb, R. (1993). “Centrifuge Modeling of Ice Scour.” 4th Canadian Conference on Marine Geotechnical Engineering, St. John's, Newfoundland, pp.356-374.
33. Lele, S.P., Hamilton, J.M., Panico, M., Arslan, H., and Minnaar, K. (2011). “3D Continuum Simulations to Determine Pipeline Strain Demand Due to Ice-Gouge Hazards.” Proc Arctic Technology Conference, Houston, Texas.
34. Lele, S.P., Hamilton, J.M., Panico, M., Arslan, H. (2011), “Advanced Continuum Modeling to Determine Pipeline Strain Demand due to Ice Gouging.” Int. Conference on Offshore and Polar Engineering, Maui, Hawaii, ISOPE, Vol. 4. ISBN 978-1-880653-96-8.
35. Liferov, P. (2005). “First-year Ice Ridge Scour and Some Aspects of Ice Rubble Behavior.” Ph.D. thesis, Norwegian Univ. of Science and Technology, Trondheim, Norway.
36. Nixon, J.R, Palmer, A., and Phillips, R. (1996). “Simulations for Buried Pipeline Deformations Beneath Ice Scour.” Offshore Marine and Arctic Engineering, Florence, Italy.
37. Nobahar, A., Phillips, R., and Zhou, J. (2004). “Trench Effects on Pipe-Soil Interaction.” Proc., 5th IPC, Paper No. IPC04-0141.
38. Nobahar, A., Kenny, S., and Phillips, R. (2007). “Buried Pipelines Subject to Subgouge Deformations.” ASCE International Journal of Geomechanics GM/2005/000235, Vol. 7, No. 3, pp.206-216.
39. O’Rourke, M. J. and Liu, X. (1995). “Lifeline Earthquake Engineering.” Proc., 4th U.S. Conf., San Francisco, Technical Council on Lifeline Earthquake Engineering, New York.
40. Panico, M., Lele, S. P., Hamilton, J. M., Arslan, H., and Cheng, W. (January 1, 2012). “Advanced Ice Gouging Continuum Models: Comparison With Centrifuge Test Results.” International Society of Offshore and Polar Engineers.

41. Peek, R. and Nobahar, A. (2012). “Ice Gouging Over a Buried Pipeline: Superposition Error of Simple Beam-and-Spring Models.” Int. J. Geomech. 12 (4), 508–516.
42. Pike, K. and Kenny, S. (2012). “Advanced Continuum Modeling of the Ice Gouge Process: Assessment of Keel Shape Effect and Geotechnical Data.” Proc., ISOPE, 6p.
43. Phillips, R., Nobahar, A., and Zhou, J. (2004). “Combined Axial and Lateral Pipe-Soil Interaction Relationships.” Proc., 5th IPC, Paper No. IPC04-0144.
44. Phillips, R., Clark, J. I., and Kenny, S. (2005). “PRISE Studies on Gouge Forces and Subgouge Deformations.” 18th Int Conf Port and Ocean Engineering Under Arctic Conditions, Vol. 1, pp. 75-84.
45. Phillips, R., Barrett, J.A., Al-Showaiter, A., (2010), “Ice Keel-Seabed Interaction: Numerical Modeling Validation.” Proc. Offshore Technology Conference, Houston, Texas.
46. Phillips, R. and Barrett, J. (2011). “Ice Keel-Seabed Interaction: Numerical Modeling for Sands.” Paper presented at the Port and Ocean Engineering Under Arctic Conditions, Montreal.
47. Rogers, B., Blasco, S., and Jefferies, M. (1993). “Pressure Meter Testing in Beaufort Shelf Surficial Sediments.” 4th Canadian Conference on Marine Geotechnical Engineering, Vol. 1, (pp. 208-228). St. John's, NL, Canada.
48. Rossiter, C. P. and Kenny, S. P. (2012). “Assessment of Ice/Soil Interactions: Continuum Modeling in Clays.” Proc., ISOPE2012, 10p.
49. Sayed, M. and Timco, G. (2009). “A Numerical Model of Iceberg Scour.” Cold Regions Sci. Tech., 55(1):103-110.
50. Schoonbeek, I.S.S. and Allersma, H.G.B. (2006). “Centrifuge Modeling Of Scouring Ice Keels in Clay.” Physical Modeling in Geotechnics – 6th ICPMG ’06 – Ng, Zhang and Wang 2006 Taylor & Francis Group, London, ISBN 0-415-41586-1.
51. Yang, Q.S., Poorooshasb, F., and Poorooshasb, H.B. (1993). “Analysis of Subscour Deformation by Finite Element Method.” 4th Canadian Conference on Marine Geotechnical Engineering. Vol.2, pp. 739-754.
52. Yang, Q.S. and Poorooshasb, H.B. (1997). “Numerical Modeling of Seabed Ice Scour.” Computers and Geotechnics, Vol.21, No. 1, pp. 1-20.
53. Zienkiewicz, O.C., M. Huang, and M. Pastor (1995). “Localization Problems in Plasticity Using Finite Elements with Adaptive Remeshing.” Intl J Numerical and Analytical Methods in Geomechanics, 19(2), pp.127-148.
54. Wang, J. and Gadala, M.S. (1997). “Formulation and Survey of ALE Method in Nonlinear Solid Mechanics.” Finite Elem. Anal. Des., 24, pp.253–269.
55. Winkler, E. (1867), “Die Leher von der Elastizitat und Festigkeit.” Dominicus, Prague Dominicus, Prague.

56. Woodworth-Lynas C., Nixon D., Phillips R., and Palmer A. (1996). “Subgouge Deformations and the Security of Arctic Marine Pipelines.” Proceedings of the 28th Offshore Technology Conference (OTC), Houston, pp. 657–664.
57. Wu, C-T, Chen, J. S., and Huck, Frank (2001). “Lagrangian Meshfree Formulation for Analysis of Geotechnical Materials.” Journal of Engineering Mechanics, Vol.127, No. 5, pp. 440-449.

-o0o-

Appendix A Glossary

A.1 Glossary Terms

ABAQUS: A software suite for Finite Element Analysis (FEA) and computer-aided engineering.

Adaptive mesh technique: A local mesh refinement strategy to improve the convergence of solution in problematic areas.

Advection: A transport mechanism of a substance or conserved property (e.g., energy) by a fluid due to the fluid's bulk motion.

Attack angle: The angle between the keel face and the contacting soil surface.

Bearing capacity: In geotechnical engineering, the capacity of soil to support the loads applied to the ground. The bearing capacity of soil is the maximum average contact pressure between the foundation and the soil which should not produce shear failure in the soil.

Boundary condition: The set of conditions specified for the behavior of the solution to a set of differential equations at the boundary of its domain. In FEA simulations, it is the restriction of a certain degree of freedom applied at the set of nodes.

Cam-Clay (CC) and Modified Cam-Clay (MCC): The first critical state models for describing the behavior of soft soils such as clay, the Cam-Clay (CC) and Modified Cam-Clay (MCC) were formulated by researchers at Cambridge University. Both models describe three important aspects of soil behavior: (i) Strength, (ii) Compression or dilatancy (the volume change that occurs with shearing), (iii) Critical state at which soil elements can experience unlimited distortion without any changes in stress or volume. A major advantage of cap plasticity models, a class to which the CC and MCC formulations belong, is their ability to model volume changes more realistically.

CAP Model (LS-DYNA): A constitutive model where shear and compaction surfaces are combined to form a smooth, continuous surface.

C-CORE: Canadian research and development (R&D) corporation.

Centrifuge modeling: Involves testing of small-scale models in the enhanced gravity field of a geotechnical centrifuge. This technique is particularly useful in testing materials such as soils that exhibit non-linear stress-strain behavior and can suffer significant plastic strains.

Constitutive modeling: The mathematical description of how materials respond to various loadings so that any increment of strain applied on a material will cause a stress increment.

Continuum approach: A material is modeled as a continuous mass, meaning the matter in the body is continuously distributed and fills the entire region of space it occupies.

Convergence: In FEA, convergence is achieved when the output from the FE program is converging on a single correct solution. To check the convergence of the solution, at least two solutions to the same problem are required. The solution from the FE program is checked with a solution of increased accuracy. If the more accurate solution is dramatically different from the original solution, then the solution is not converged. However, if the solution does not change much (less than a few percentage points of difference), then the solution is considered converged.

Critical state: This state is reached when the soil distorts at a constant state of stress with no volume change. This state is characterized by the Critical State Line (CSL).

Dead wedge: Soil mass in the frontal mount that doesn't undergo significant displacements during ice gouging and remains 'attached' to the keel.

Dilatancy: The observed tendency of a compacted granular material to dilate (expand in volume) as it is sheared. This occurs because the grains in a compacted state are interlocking and therefore do not have the freedom to move around one another. When stressed, a lever motion occurs between neighboring grains, which produces a bulk expansion of the material. On the other hand, when a granular material starts in a very loose state, it may initially compact instead of dilating under shear.

Dilation angle: Controls an amount of plastic volumetric strain developed during plastic shearing and is assumed constant during plastic yielding.

Drained condition: Occurs when there is no change in pore water pressure due to external loading. In a drained condition, the pore water can drain out of the soil easily, causing volumetric strains in the soil.

Drucker–Prager: A failure criterion that is a three-dimensional pressure-dependent model to estimate the stress state at which soil reaches its ultimate strength.

Friction angle φ: The strength of sand is usually characterized by the peak friction angle υ and the critical state friction angle υ_c. It is generally realized that the peak friction angle depends not only on density but also on the stress path.

Iceberg: Ice that has broken off from glaciers or shelf ice and is floating in open water. To be classified as an iceberg, the height of the ice must be greater than 16 ft. above sea level, the thickness must be 98 – 164 ft., and the ice must cover an area of at least 5,382 square ft.

Isoparametric formulation: Allows elements to be created that are nonrectangular and have curved sides.

Keel: The submerged counterpart of an ice ridge/iceberg.

Lach's experiment: Lach conducted centrifuge experiments in Cambridge University's geotechnical centrifuge in 1992. He is thought to be one of the pioneers in the study of ice gouging. Test 05 was the base case for the experimental program, where the keel attack angle was set to 15°, keel width was 0.328 ft. (100 mm) or 32.8 ft. at prototype scale, and the steady state gouge depth attained was 0.039 ft. (12.1 mm) or 0.39 at prototype scale. Many later researchers have referred to Lach's experiments and compared results of numerical simulations with his.

Limit State Design (LSD): Also known as Load and Resistance Factor Design (LRFD), refers to a design method used in structural engineering. A limit state is a condition of a structure beyond which it no longer fulfils the relevant design criteria. The condition may refer to a degree of loading or other actions on the structure, while the criteria refer to structural integrity, fitness for use, durability, or other design requirements

Mesh distortion: Deformations alter the FE mesh, often to the point where the mesh is unable to provide accurate results or the analysis terminates for numerical reasons. In such simulations it is necessary to use adaptive meshing tools to periodically minimize the distortion in the mesh. Mohr Coulomb describes a linear relationship between normal and shear stresses (or maximum and minimum principal stresses) at failure and combines Hooke's Law with Coulomb's failure criteria for shear strength.

Nonlinear spring: An element that has a defined nonlinear load-displacement function.

Penalty methods: A certain class of algorithms for solving constrained optimization problems. A penalty method replaces a constrained optimization problem by a series of unconstrained problems whose solutions ideally converge to the solution of the original constrained problem. The unconstrained problems are formed by adding a term, called a penalty function.

PRISE (Pressure Ridge Ice Scour Experiment): This joint industry research program investigated the stresses and soil deformations during ice gouging events. It was a proprietary program designed to develop the engineering framework to allow pipeline installation in arctic regions. The program included a series of small-scale physical tests conducted in a geotechnical centrifuge to enhance the understanding of soil deformations and ice loads that occur during ice gouging events.

Ramberg–Osgood: This equation was created to describe the nonlinear relationship between stress and strain—that is, the stress–strain curve—in materials near their yield points. It is especially useful for metals that harden with plastic deformation (strain hardening), showing a smooth elastic-plastic transition.

Reliability: Theoretically defined as the probability of success (Reliability = 1 - Probability of Failure), as the frequency of failures, or in terms of availability, as a probability derived from reliability and maintainability. Reliability engineering deals with the estimation and management of high levels of 'lifetime' engineering uncertainty and risks of failure.

Shell elements: 4- to 8-node isoparametric quadrilaterals or 3- to 6-node triangular elements in any 3-D orientation.

Soil resistance: The pressure exerted by the soil against a structure on a surface of a surrounding soil mass. It can be classified as earth pressure at rest, active resistance, and **passive resistance**. When a soil mass pushes against a structure, the pressure is known as active pressure. On the other hand, if the retaining structure pushes against the soil mass, the resulting pressure is known as passive pressure.

Stain gradient: An increase or decrease in the magnitude of strain observed in passing from one point or moment to another.

Steady state gouging: A gouging ice keel is thought to have reached steady state when the frontal mount and side berms have reached their ultimate sizes.

Strain contour: Mapping of points with the same amplitude of strain in a continuous line or surface.

Strain localization/Shear band: A narrow zone of intense shearing strain, usually of plastic nature, developing during severe deformation of ductile materials.

Subgouge deformation profile: The magnitude and extent of deformations taking place underneath the gouging keel.

T-bar test: Test used in site investigations to obtain accurate intact and remolded undrained strength profiles of soft sediments.

Total stress analysis: Analysis that uses the undrained shear strength of the soil. The total stress analysis is typically only used for cohesive soil. The total stress analysis is often used for the evaluation of foundations and embankments to be supported by cohesive soil. The actual analysis is performed for rapid loading or unloading conditions often encountered during the construction phase or just at the end of construction. This analysis is applicable to field situations where there is a change in shear stress which occurs quickly enough that the cohesive soil does not have time to consolidate, or in the case of heavily overconsolidated cohesive soils, the negative pore water pressures do not have time to dissipate.

Undrained condition: Condition that occurs when the pore water is unable to drain out of the soil. In an undrained condition, the rate of loading is much quicker than the rate at which the pore water is able to drain out of the soil. As a result, most of the external loading is taken by the pore water, resulting in an increase in the pore water pressure. The tendency of soil to change volume is suppressed during undrained loading.

Undrained Shear strength (Su): A term used in soil mechanics to describe the magnitude of the shear stress that a soil can sustain under undrained conditions.

Von Mises criterion: This constitutive model considers piecewise linear elasto-perfectly plastic soil behavior with yield strength independent of hydrostatic pressure. In terms of simulating cohesive soil behavior, the classical plasticity model assumes fully saturated conditions with undrained loading (i.e., total stress). The von Mises yield surface in principal stress space is a right cylinder and is represented by the equation of a circle in the deviatoric plane.

Winker springs: The first springs used for foundation design. The soil was treated as a row of independent springs called Winker springs, implying that the soil resistance to a settlement y would be proportional to a spring constant (stiffness). This method is also called p-y curve and is mentioned in API and DNV codes.